

Concert Hall Impulse Responses — Pori, Finland: Analysis results

Juha Merimaa¹, Timo Peltonen², and Tapio Lokki³

`juha.merimaa@hut.fi, timo.peltonen@akukon.fi, tapio.lokki@hut.fi`

¹Laboratory of Acoustics and Audio Signal Processing
Helsinki University of Technology
P.O.Box 3000, FI-02015 TKK, Finland

²Akulon Oy Consulting Engineers
Kornetintie 4 A, FI-00380 Helsinki, Finland

³Telecommunications Software and Multimedia Laboratory
Helsinki University of Technology
P.O.Box 5400, FI-02015 TKK, Finland

May 6, 2005

1 Introduction

This document presents analysis results of a published set of concert hall impulse responses. For a detailed description of the hall, measurement positions, sound sources and microphones, as well as the measurement procedure and post processing of the responses, see the reference document (Merimaa et al., 2005). The responses and all documentation are available for download from <http://www.acoustics.hut.fi/projects/poririrs/>.

A major part of this document consists of individual analysis results for each pair of source-receiver positions. The results include standard room acoustical parameters, spectrogram plots and special directional analysis of the responses. The document is organized as follows. Section 2 describes computation and purpose of the listed room acoustical parameters and Section 3 introduces the two types of figures used to illustrate the responses. The results for the individual responses have been collected to the end of the document, each source-receiver combination being presented on its own page.

2 Room acoustical parameters

The room acoustical parameters are a very traditional way of characterizing rooms or concert halls. There is some controversy in the literature describing the relation of these parameters to the actual perception of a listener. Nevertheless, the following subsections try to give some guidelines for established interpretation of the results. In order to limit the analysis, we have only chosen to present standardized parameters (ISO 3382, 1997) with the addition of Gade's (1989a; 1989b; 1992) support, describing the ability of a musician to hear him/herself when performing on the stage.

All parameters reported in this document have been calculated at octave bands. The filtering has been performed using ANSI S1.1-1986 standard filters as implemented in the Octave Matlab toolbox (Couvreur, 1997). Except for the spatial parameters interaural cross-correlation and lateral

	125 Hz	250 Hz	500 Hz	1 kHz	2 kHz	4 kHz	8 kHz
T_{30} (s)	2.7	2.5	2.4	2.4	2.1	1.7	1.2
EDT (s)	2.5	2.4	2.4	2.3	2.0	1.6	0.9
G (dB)	8.9	8.7	8.9	9.6	9.9	8.2	4.3
C_{80} (dB)	-0.3	-3.6	-3.1	-1.8	-0.6	1.6	6.6
$1 - \text{IACC}_E$	0.10	0.26	0.74	0.74	0.74	0.73	-
$1 - \text{IACC}_L$	0.12	0.31	0.87	0.89	0.94	0.94	-
LF_P	0.24	0.24	0.28	0.37	0.34	0.41	-
LF_{SF}	0.37	0.33	0.34	0.37	0.48	0.59	-
SNR (dB)	66.1	65.7	67.3	72.0	74.3	74.2	70.5

Table 1: Room acoustical parameters at octave bands averaged over all responses with receiver positions in the audience area.

energy fraction, all other parameters are reported as an average of the values derived from both of the DPA 4006 microphones.

All parameters except the signal-to-noise ratio (SNR, which is actually not a room acoustical parameter but describes the measurements) have been calculated from the denoised responses (see Merimaa et al., 2005, Section 5.1). This can be motivated as follows: Examination of the achieved SNRs and start times of the denoising process reveals that the parameters that are evaluated over a limited decay or period of time include in all cases only measured data. This leaves only strength and clarity, where the computation of energy of the whole impulse response includes the extrapolated parts. However, the denoising process extrapolates the responses in such a way, that the strength and clarity over the denoised responses are actually better estimates of the real parameters than using just the measured parts would yield.

The average parameters over all responses with receivers positions in the audience area are listed in Table 1. This is the most appropriate way to characterize the hall itself. The parameters for the individual source-receiver pairs presented in the end of this document should not be interpreted too strictly. It has been shown that the parameters can vary considerably between individual locations or even small displacements of measurement positions in a hall (Pelorsor et al., 1992; Bradley, 1994; Nielsen et al., 1998; Okano et al., 1998; de Vries et al., 2001), although it is common to assume that the perception of a hall does not vary as much within the hall.

In the following subsections, each reported parameter and the applied computation methods are described.

2.1 Reverberation time and early decay time

The reverberation time (RT) is the oldest and most common parameter describing concert hall acoustics. It is defined as the time that it takes for the sound inside a hall to decay 60 dB after a source is turned off. Similarly, the early decay time (EDT) is defined as the time during which the first 10 dB of the decay process occurs, multiplied by six.

In a perfectly diffuse hall, EDT and RT would always yield exactly the same values. In practice they do, however, differ to some degree, and EDT is more dependent on the geometry of a hall and on the measurement position (Barron, 1995). Both RT and EDT affect the subjective sense of reverberance or liveness of a hall. EDT is considered a better descriptor for the running reverberance, since during continuous sound most of the reverberation tail is masked by the sound itself. Only when there is a longer break in the source signal, a listener will be able to hear the full decay characterized by the RT.

According to Beranek (1996) the subjective reverberance is mainly determined by reverberation time at mid and high frequencies above approximately 350 Hz. On the other hand, low frequency reverberation creates a sense of warmth, which is more of a timbral attribute. Furthermore, excess-

sive low frequency reverberation can make a hall sound boomy. For describing the warmth, Beranek (1996) has proposed bass ratio defined as the ratio of average of RTs at the 125 and 250 Hz octave bands to that at 500 and 1000 Hz. Gade (1989b) has proposed a similar measure computed from EDTs at 250 and 500 Hz related to EDTs at 1 and 2 kHz.

The standard (ISO 3382, 1997) allows several ways to measure RT and EDT. We have chosen to derive them from a least-squares line fit to backward integrated squared impulse responses, which gives an ensemble average of the decay curves that would be obtained with random noise samples as an excitation (Schroeder, 1965). The RT and EDT are calculated from the slope of the fitted line. For determining the RT, the line was fitted between -5 and -35 dB points, which gives the standardized T_{30} value (ISO 3382, 1997), and for EDT between 0 and -10 dB points relative to the level of the direct sound.

2.2 Strength

The strength factor G is a parameter describing the amount of sound energy directed to a listening position. It is defined as the logarithmic ratio of the total energy of a measured response to that produced by the same sound source with the same excitation at a distance of 10 m in a free field (ISO 3382, 1997). In addition to specific acoustical features of a hall, strength depends on the distance from the sound source, as well as on the reverberation time (Barron and Lee, 1988). Perceptually the strength (especially at mid-frequencies 500 and 1000 Hz, Beranek 1996) determines the loudness of a hall. As a spectral parameter, the strength at different frequency bands is, of course, also related to the timbre.

Given the applied level calibration (Merimaa et al., 2005, Section 4.3), computation of the strength is straightforward. The total energy at each octave band was divided by the energy of the impulse response of the corresponding filter, and 10 dB was added to the resulting value.

2.3 Clarity

The clarity index is defined as the ratio of early energy to the late (reverberant) energy expressed in decibels (ISO 3382, 1997). In the clarity index C_{80} , the response is divided into the early and late parts at 80 ms after the arrival of the direct sound. Clarity is highly correlated with the decay parameters RT and EDT¹ and it also depends on the distance from the sound source somewhat similar to G (Barron and Lee, 1988; Barron, 1995). The clarity is related to the perception of what Beranek (1996) calls horizontal definition, defined as “the degree to which sounds that follow one another stand apart”.

The C_{80} values presented in this paper were calculated such that the responses were divided into early and late part before the octave band filtering. This way the time-domain spreading due to the filtering does not affect the division.

2.4 Interaural cross-correlation and lateral energy fraction

Interaural cross-correlation (IACC) and lateral energy fraction (LF) are related to the spatial properties of a hall. IACC can be calculated from impulse responses measured with a dummy or a real head and it is defined as the maximum of the normalized interaural cross-correlation function over lags in the range of $[-1, 1]$ ms (ISO 3382, 1997). IACC is typically divided into $IACC_E$ integrated over 0–80 ms from the arrival of the direct sound and to $IACC_L$ integrated over 80–1000 ms (Bradley, 1994; Hidaka et al., 1995). For determining the LF, an omnidirectional and a figure-of-eight microphone are needed. LF is defined as the fraction of the energy arriving from lateral directions during the early part of a response (0–80 ms) (ISO 3382, 1997).

The IACC and LF are intended as measures of spatial impression. The spatial impression is typically divided into auditory source width (ASW) and listener envelopment (LEV). ASW depends

¹The correlation is especially high between C_{80} and the ratio of RT and EDT (Barron, 1995).

mainly on the early reflections characterized by IACC_E and LF, whereas the envelopment is created by diffuse late reverberation as measured with IACC_L (Morimoto and Maekawa, 1989; Bradley and Soulodre, 1995a)². Okano et al. (1998) have proposed the average of $[1 - \text{IACC}_E]$ over the octave bands centered at 500, 1000, and 2000 Hz combined with strength at frequencies below 125 Hz as the best descriptors for ASW. However, despite the established nature of these parameters, they do not always seem to be able to describe the perception, when acoustical environments of considerably different size are compared (Merimaa and Hess, 2004).

At low frequencies the $[1 - \text{IACC}_E]$ values are always low since the relatively small distance between the ears of the dummy head compared to the wavelength of sound results in a high correlation. Nevertheless, at octave bands up to 1 kHz, the hall averages of $[1 - \text{IACC}_E]$ and LF have been shown to correlate strongly (Bradley, 1994). With increasing frequency, IACC gains more sensitivity to sound emanating from directions closer to the median plane than the (ideally) frequency independent figure-of-eight directivity pattern used in LF. According to Okano et al. (1998) IACC_E describes the human spatial perception better than LF when these two parameters disagree.

The IACC values reported in this paper were computed from the non-diffuse-field-equalized dummy head responses and they are reported in the form $[1 - \text{IACC}]$ such that high values describe high diffuseness (low correlation).

The LF estimates were derived both from measurements with the Pearl TL-4 stereo back-to-back cardioid microphone (LF_P) and the SoundField microphone system (LF_{SF}). The omnidirectional energy was integrated over 0–80 ms and the lateral energy over 5–80 ms to exclude possible leakage of the direct sound into the lateral signal (ISO 3382, 1997). With the Pearl microphone, the responses of the left and right channels were subtracted from one another to obtain the figure-of-eight directivity pattern and summed to obtain the omnidirectional reference response. In case of the SoundField microphone, both directivity patterns were readily available, but the utilized figure-of-eight channel Y was scaled by $1/\sqrt{2}$ to compensate for the B-format gain convention. It is interesting to notice that the results differ considerably. Part of these differences may be due to nonideal directivity patterns of the microphones. Furthermore, measurements of a SoundField MKV system (Farina, 2001) have shown another source of error caused by frequency dependent variations in the relative gains of the omnidirectional and figure-of-eight channels. This result leads the authors to believe that the LF_P values are more reliable.

2.5 Support

Support (ST) aims at describing a hall from a performing musician's point of view. The ST parameters were developed to describe the perceptual support, which is "the property which makes the musician feel that he can hear himself and that it is not necessary to force the instrument to develop the tone" (Gade, 1989a).

ST is defined as the ratio of reflected energy to the emitted energy, as measured with an omnidirectional microphone at a distance of 1 m from a sound source on the stage. The emitted energy is integrated over the time interval of 0–10 ms after the arrival of the direct sound, including typically the direct sound and the first floor reflection. For computing the reflected energy, Gade (1989a,b) proposed originally two time intervals: 20–100 ms (ST1) and 20–200 ms (ST2). In a later publication (Gade, 1992), ST1 was renamed ST_{early} and ST_{late} including reflected energy integrated over 100–1000 ms was introduced. Furthermore, ST2 was replaced by ST_{total} , which can be calculated as the (linear) sum of ST_{early} and ST_{late} .

The ST_{early} and ST_{late} values for the three source positions are listed in Table 2. These parameters were calculated from responses which were excluded from the public database due to little use for anything apart from the support calculation. The responses were measured with the DPA 4006 microphone pair at a distance of 1 m from each source position and the parameters computed from

²Bradley and Soulodre (1995b) have also proposed late lateral energy (as opposed to energy fraction) for measuring envelopment.

	ST _{early}				
	250 Hz	500 Hz	1 kHz	2 kHz	4 kHz
S1	-14.1	-12.7	-11.3	-10.3	-9.9
S2	-11.8	-9.7	-10.5	-8.3	-5.1
S3	-12.3	-9.0	-10.5	-9.2	-8.7
Avg.	-12.6	-10.2	-10.7	-9.2	-7.4

	ST _{late}				
	250 Hz	500 Hz	1 kHz	2 kHz	4 kHz
S1	-11.2	-12.1	-12.0	-10.4	-10.6
S2	-13.2	-12.0	-11.7	-11.3	-9.9
S3	-14.6	-12.7	-11.9	-11.6	-12.1
Avg	-12.8	-12.3	-11.9	-11.1	-10.8

Table 2: Support (in dB) at each source position.

both microphones were averaged. Only the omnidirectional sound source (as opposed to having also a subwoofer) was used and for this reason the ST at the 125 Hz octave band has been omitted from the results. Furthermore, the source cannot be considered omnidirectional at the omitted 8 kHz octave band and the listed 4 kHz results should also be interpreted with some care while the results are prone to random errors depending on the direction of the measurement position relative to the sound source.

2.6 Signal-to-noise ratio

As mentioned earlier, signal-to-noise ratio (SNR) is actually not a room acoustical parameter but describes the measurements. The listed SNR values were calculated as the ratio of the peak value of a response to the background noise level averaged over 10 % of the end of a response prior to denoising. The DPA 4006 responses were used, and in each case it was verified that the 10 % of the samples were indeed background noise.

3 Figures

The figures presented for each source-receiver pair in the end of this document consist of spectrograms and a special directional analysis of the early responses.

3.1 Spectrograms

The spectrograms provide a time-frequency representation of the decay of a response. They were calculated from the rightmost (reference) DPA 4006 microphone measurements after applying the denoising procedure (Merimaa et al., 2005, Section 5.1). The computation was performed using 1024 sample FFT with 50 % overlapping Hann windowed time frames. The resolution is thus the same as that used in the denoising. The energy of each time-frequency component is plotted on a dB scale. The frequency range of the plots has been limited to 20 kHz and the spectrograms are presented over the full length of the waveform files in the database. Furthermore, the frequency-dependent starting point of the extrapolated exponentially decaying random noise created in the denoising process is shown with a solid black line on top of the spectrograms.

3.2 Directional analysis

The directional analysis plots illustrate the direction dependent arrival of sound to a measurement position during a time period of 100 ms starting from slightly before the arrival of the direct sound.

The figures consist of a time-frequency representation of active sound intensity plotted on top of an omnidirectional sound pressure spectrogram (Merimaa et al., 2001). The active intensity is a vector quantity describing the net flow of sound energy within an analysis window. For the visualization, the three-dimensional vectors have been projected into two two-dimensional planes: the horizontal plane and the median plane. In both planes, vectors pointing to the right represent sound emanating from the front direction (as defined in Merimaa et al., 2005, Section 3.2). In the horizontal plane a vector pointing down signifies sound arriving from the right side, and in the median plane a vector pointing down represents sound arriving from above.

Both the active intensity and the spectrograms have been computed from 128 sample long Hann windowed time frames. The time-frequency representations have been adjusted for illustrational purposes. Zero-padding and largely overlapping windows have been used to smooth the spectrogram, and the intensity vectors are plotted only for positions of local maxima as a function of time. Furthermore, the data have been thresholded to levels shown in the color bars of the figures in order to highlight the strongest reflections. The lengths of the vectors are proportional to the component of the logarithmic magnitude of the sound intensity in the plane in question, and the underlying spectrograms are also displayed on a logarithmic (dB) scale.

Two different microphone systems have been used in the directional analysis. For the receiver positions in the audience area, the figures were calculated from measurements that were not included in the public database. The measurements were performed with a custom microphone array consisting of 12 Sennheiser KE 4-211-2 omnidirectional electret microphone capsules arranged as two pairs on each Cartesian coordinate axis. The existence of two concentric pairs with different spacings on each axis increases the reliability of the results and makes it possible to extend the analysis to a wider frequency range than with the SoundField microphone system. However, similar analysis can be performed with the SoundField microphone and this was done for the receiver positions on the stage, where the custom array was not used.

The directional analysis is identical to part of the analysis performed in the Spatial Impulse Response Rendering (SIRR) method (Merimaa et al., 2005, Section 5.3). For details of the analysis procedure with the custom array, see (Merimaa et al., 2001; Merimaa, 2002) and with a SoundField microphone (Merimaa and Pulkki, 2004, 2005). In this document the results are shown for a frequency range of 100–10000 Hz for the custom array, and 100–5000 Hz for the SoundField microphone system.

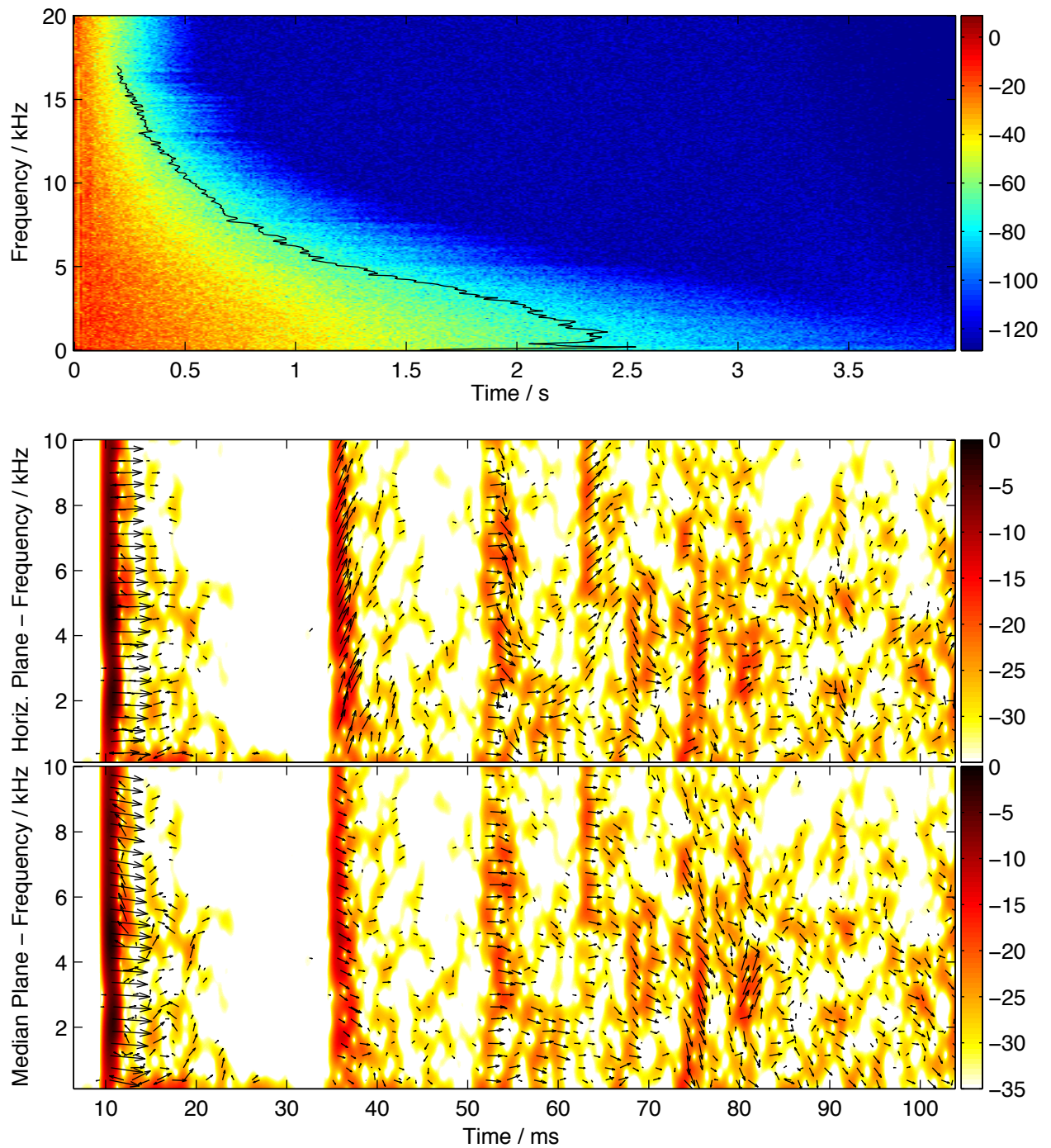
References

- M. Barron. Interpretation of early decay times in concert auditoria. *Acustica*, 81:320–331, 1995.
- M. Barron and L.-J. Lee. Energy relations in concert auditoriums. I. *J. Acoust. Soc. Am.*, 84(2):618–628, 1988.
- L. L. Beranek. *Concert and Opera Halls — How They Sound*. Acoustical Society of America, Woodbury, NY, USA, 1996.
- J. S. Bradley. Comparison of concert hall measurements of spatial impression. *J. Acoust. Soc. Am.*, 96(6):3525–3535, 1994.
- J. S. Bradley and G. A. Soulodre. The influence of late arriving energy on spatial impression. *J. Acoust. Soc. Am.*, 97(4):2263–2271, 1995a.
- J. S. Bradley and G. A. Soulodre. Objective measures of listener envelopment. *J. Acoust. Soc. Am.*, 98(5):2590–2597, 1995b.
- C. Couvreur. Octave, 1997. Matlab toolbox, available at MathWorks File Exchange central <http://www.mathworks.com/matlabcentral/fileexchange/>.

- D. de Vries, E. M. Hulsebos, and J. Baan. Spatial fluctuations in measures for spaciousness. *J. Acoust. Soc. Am.*, 110(2):947–954, 2001.
- A. Farina. Anechoic measurement of the polar plots of a Soundfield MKV B-format microphone. <http://pcfarina.eng.unipr.it/Public/Soundfield/MKV-PolarPatterns.PDF>, 2001.
- A. C. Gade. Investigations of musicians' room acoustic conditions in concert halls. Part I: Methods and laboratory experiments. *Acustica*, 69:193–203, 1989a.
- A. C. Gade. Investigations of musicians' room acoustic conditions in concert halls. Part II: Field experiments and synthesis of results. *Acustica*, 69:249–262, 1989b.
- A. C. Gade. Practical aspects of room acoustic measurements on orchestra platforms. In *Proc. 14th International Congress on Acoustics*, Beijing, China, 1992. Paper F3-5.
- T. Hidaka, L. L. Beranek, and T. Okano. Interaural cross-correlation, lateral fraction, and low- and high-frequency sound level measures of acoustical quality in concert halls. *J. Acoust. Soc. Am.*, 98(2):988–1007, 1995.
- ISO 3382. Acoustics — Measurement of the reverberation time of rooms with reference to other acoustical parameters. International Standards Organization, 1997.
- J. Merimaa. Applications of a 3-D microphone array. In *AES 112th Convention*, Munich, Germany, 2002. Preprint 5501.
- J. Merimaa and W. Hess. Training of listeners for evaluation of spatial attributes of sound. In *AES 117th Convention*, San Francisco, CA, USA, 2004. Preprint 6237.
- J. Merimaa, T. Lokki, T. Peltonen, and M. Karjalainen. Measurement, analysis, and visualization of directional room responses. In *AES 111th Convention*, New York, NY, USA, 2001. Preprint 5449.
- J. Merimaa, T. Peltonen, and T. Lokki. Concert hall impulse responses — Pori, Finland: Reference, 2005. Available at <http://www.acoustics.hut.fi/projects/poririrs/>.
- J. Merimaa and V. Pulkki. Spatial Impulse Response Rendering. In *Proc. 7th International Conference on Digital Audio Effects*, pages 139–144, Naples, Italy, 2004.
- J. Merimaa and V. Pulkki. Spatial Impulse Response Rendering I: Analysis and synthesis. *J. Audio Eng. Soc.*, 2005. Submitted in February.
- M. Morimoto and Z. Maekawa. Auditory spaciousness and envelopment. In *Proc. 13th International Congress on Acoustics*, volume 2, pages 215–218, Yugoslavia, 1989.
- J. L. Nielsen, M. M. Halstead, and A. H. Marshall. On spatial validity of room acoustics measures. In *Proc. 16th International Congress on Acoustics*, pages 2141–2142, Seattle, WA, USA, 1998.
- T. Okano, L. L. Beranek, and T. Hidaka. Relations among interaural cross-correlation coefficient ($IACC_E$), lateral fraction (LFE), and apparent source width (ASW) in concert halls. *J. Acoust. Soc. Am.*, 104(1):255–265, 1998.
- X. Pelorson, J.-P. Vian, and J.-D. Polack. On the variability of room acoustical parameters: Reproducibility and statistical validity. *Appl. Acoust.*, 37(3):175–198, 1992.
- M. R. Schroeder. New method for measuring reverberation time. *J. Acoust. Soc. Am.*, 37(3):409–412, 1965.

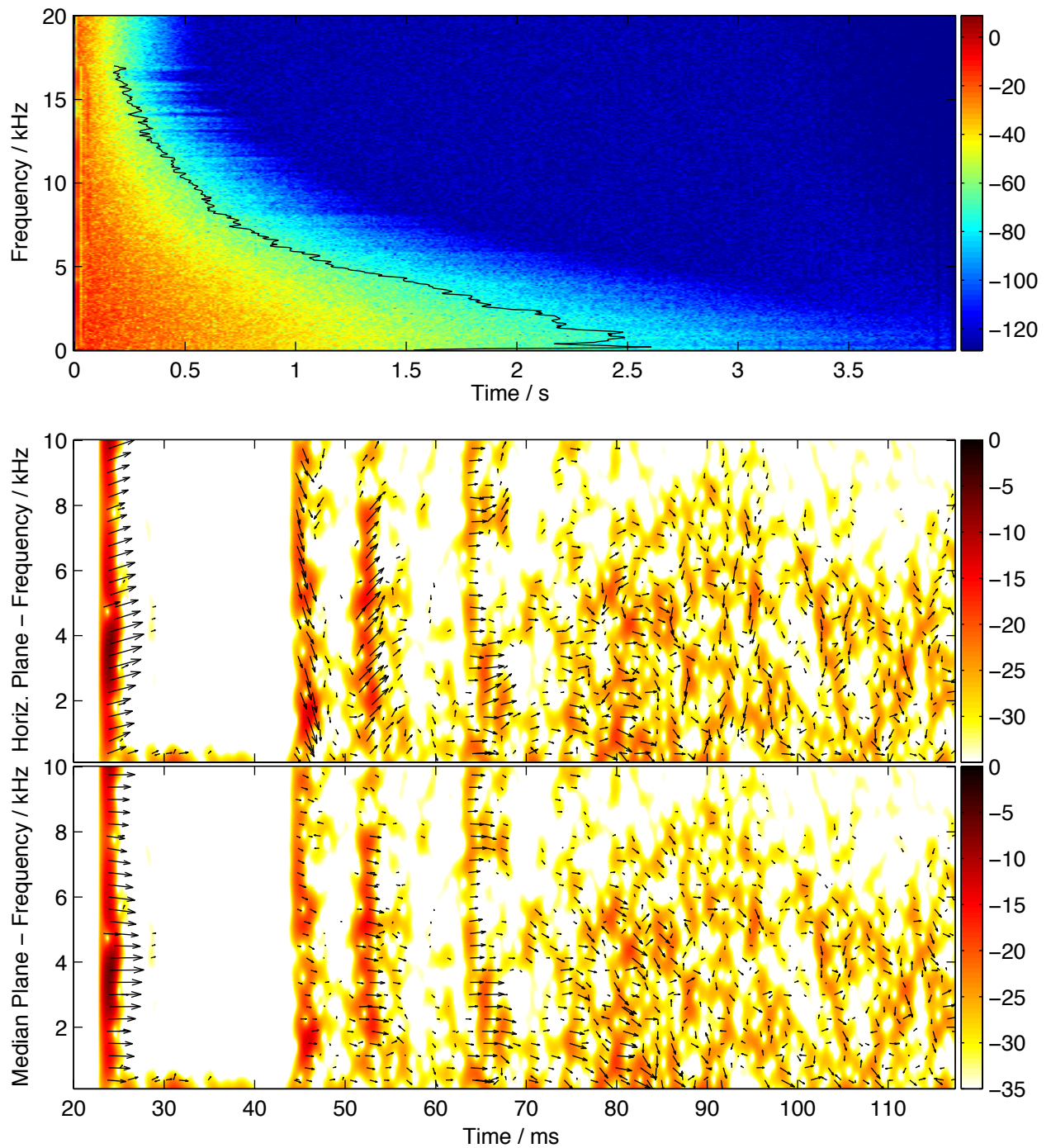
S1–R1

	125 Hz	250 Hz	500 Hz	1 kHz	2 kHz	4 kHz	8 kHz
T_{30} (s)	2.7	2.4	2.4	2.3	2.1	1.7	1.1
EDT (s)	1.8	2.5	2.2	2.2	1.8	1.5	0.9
G (dB)	11.8	10.0	10.7	11.6	11.8	9.1	9.1
C_{80} (dB)	2.2	-1.6	-0.7	-0.1	0.6	0.8	10.0
$1 - \text{IACC}_E$	0.09	0.34	0.48	0.52	0.35	0.23	-
$1 - \text{IACC}_L$	0.17	0.35	0.92	0.91	0.93	0.93	-
LF_P	0.14	0.22	0.16	0.18	0.17	0.16	-
LF_{SF}	0.20	0.15	0.11	0.20	0.31	0.79	-
SNR (dB)	68.4	64.8	73.1	79.8	78.1	76.1	77.2



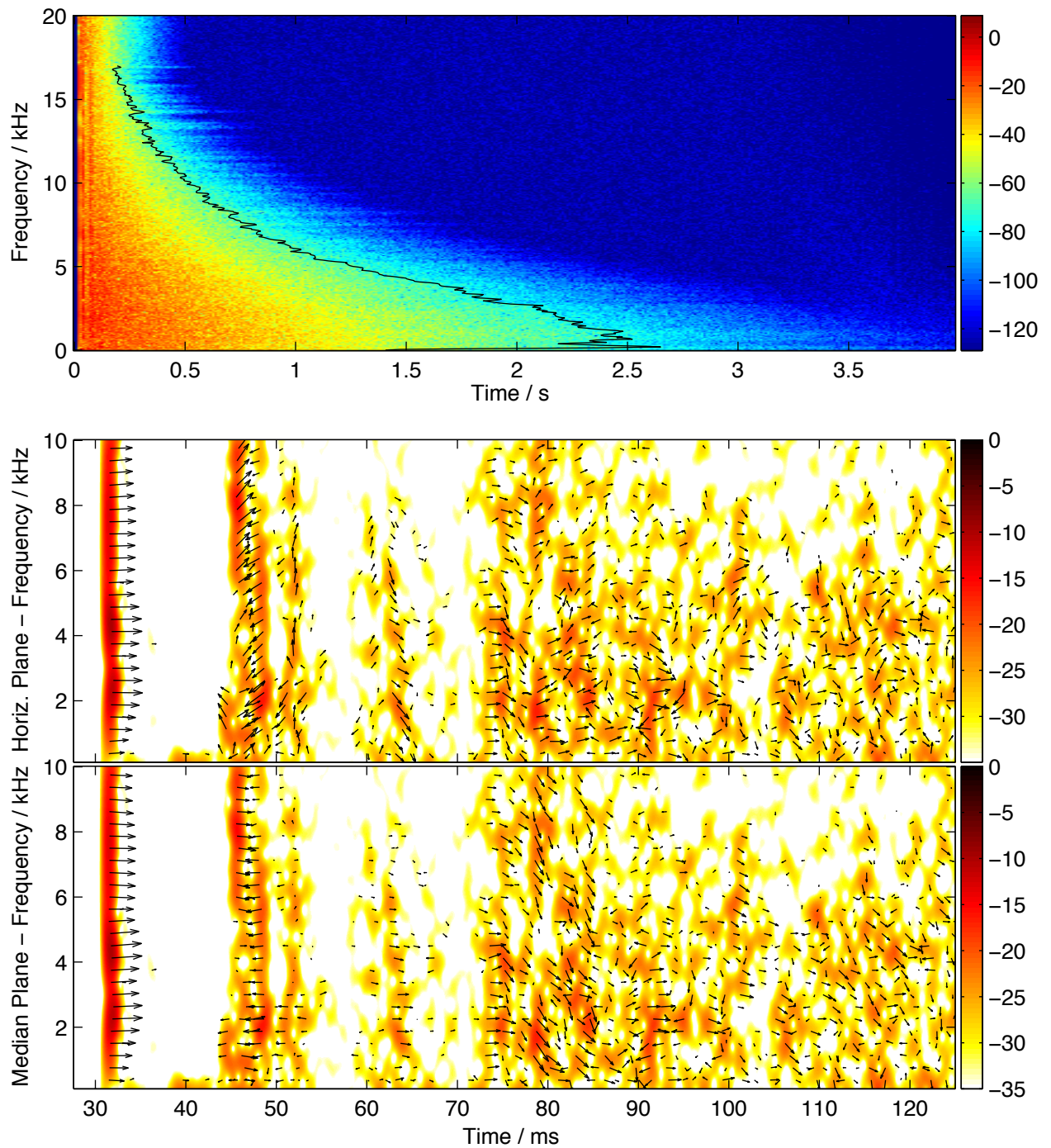
S1–R2

	125 Hz	250 Hz	500 Hz	1 kHz	2 kHz	4 kHz	8 kHz
T_{30} (s)	2.6	2.4	2.4	2.3	2.1	1.7	1.2
EDT (s)	2.5	2.5	2.3	2.4	2.0	1.7	1.0
G (dB)	9.7	8.5	9.7	9.8	10.0	7.9	3.3
C_{80} (dB)	1.7	-4.7	-2.5	-1.8	-1.2	0.5	4.1
$1 - \text{IACC}_E$	0.05	0.21	0.67	0.65	0.80	0.75	-
$1 - \text{IACC}_L$	0.16	0.32	0.93	0.85	0.92	0.92	-
LF_P	0.14	0.25	0.26	0.32	0.40	0.42	-
LF_{SF}	0.26	0.35	0.39	0.45	0.38	0.42	-
SNR (dB)	68.9	63.6	66.6	72.5	77.3	74.5	69.7



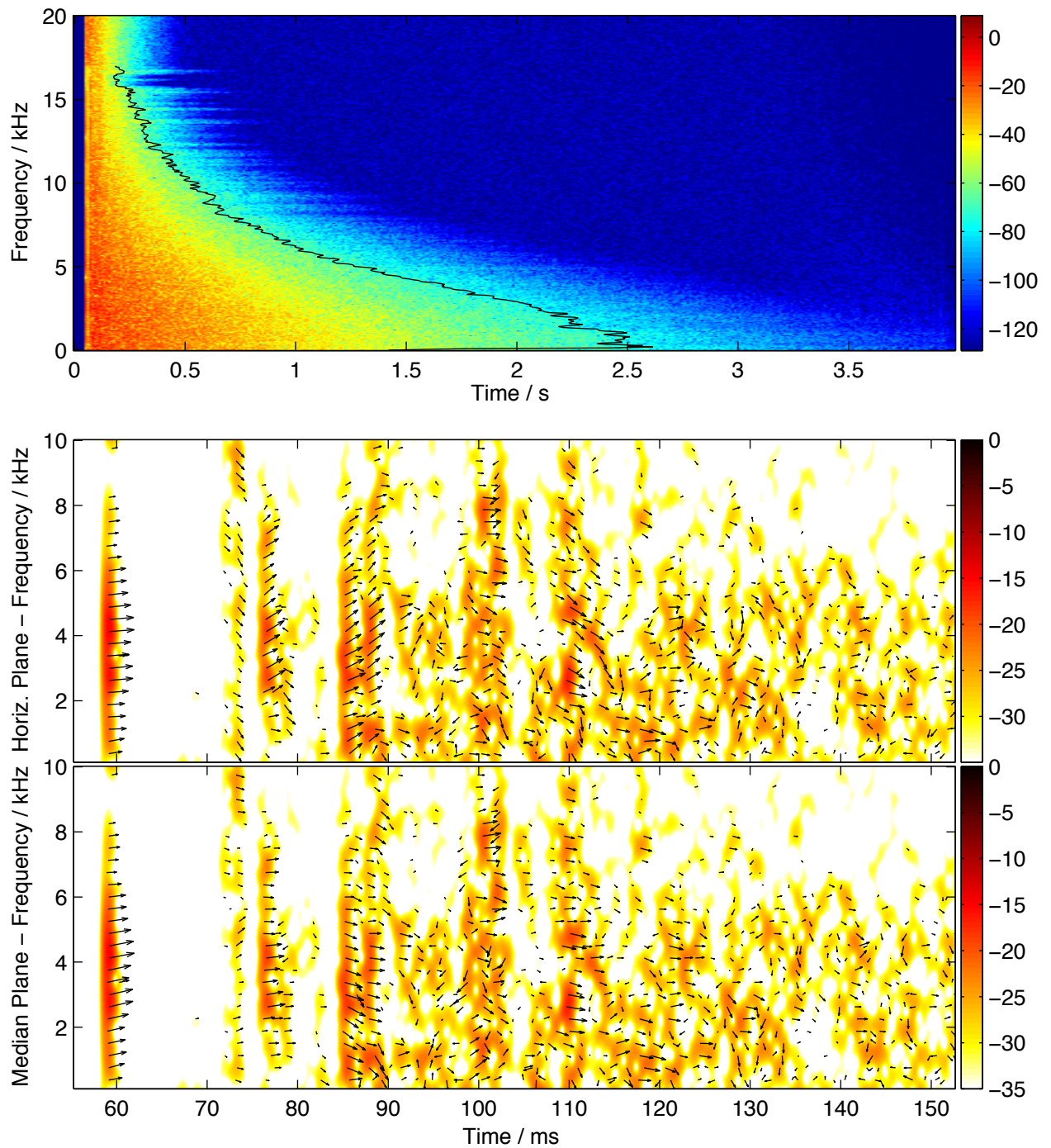
S1–R3

	125 Hz	250 Hz	500 Hz	1 kHz	2 kHz	4 kHz	8 kHz
T_{30} (s)	2.8	2.5	2.4	2.4	2.1	1.7	1.2
EDT (s)	2.4	2.2	2.5	2.3	1.9	1.5	0.9
G (dB)	8.5	9.1	8.7	9.7	10.1	8.5	2.9
C_{80} (dB)	-0.2	-7.0	-4.6	-1.9	-1.3	1.1	4.7
$1 - \text{IACC}_E$	0.14	0.26	0.83	0.74	0.82	0.87	-
$1 - \text{IACC}_L$	0.10	0.24	0.87	0.78	0.94	0.94	-
LF_P	0.28	0.25	0.25	0.47	0.41	0.68	-
LF_{SF}	0.34	0.23	0.38	0.30	0.47	0.58	-
SNR (dB)	62.4	69.3	65.6	69.7	73.0	74.5	65.7



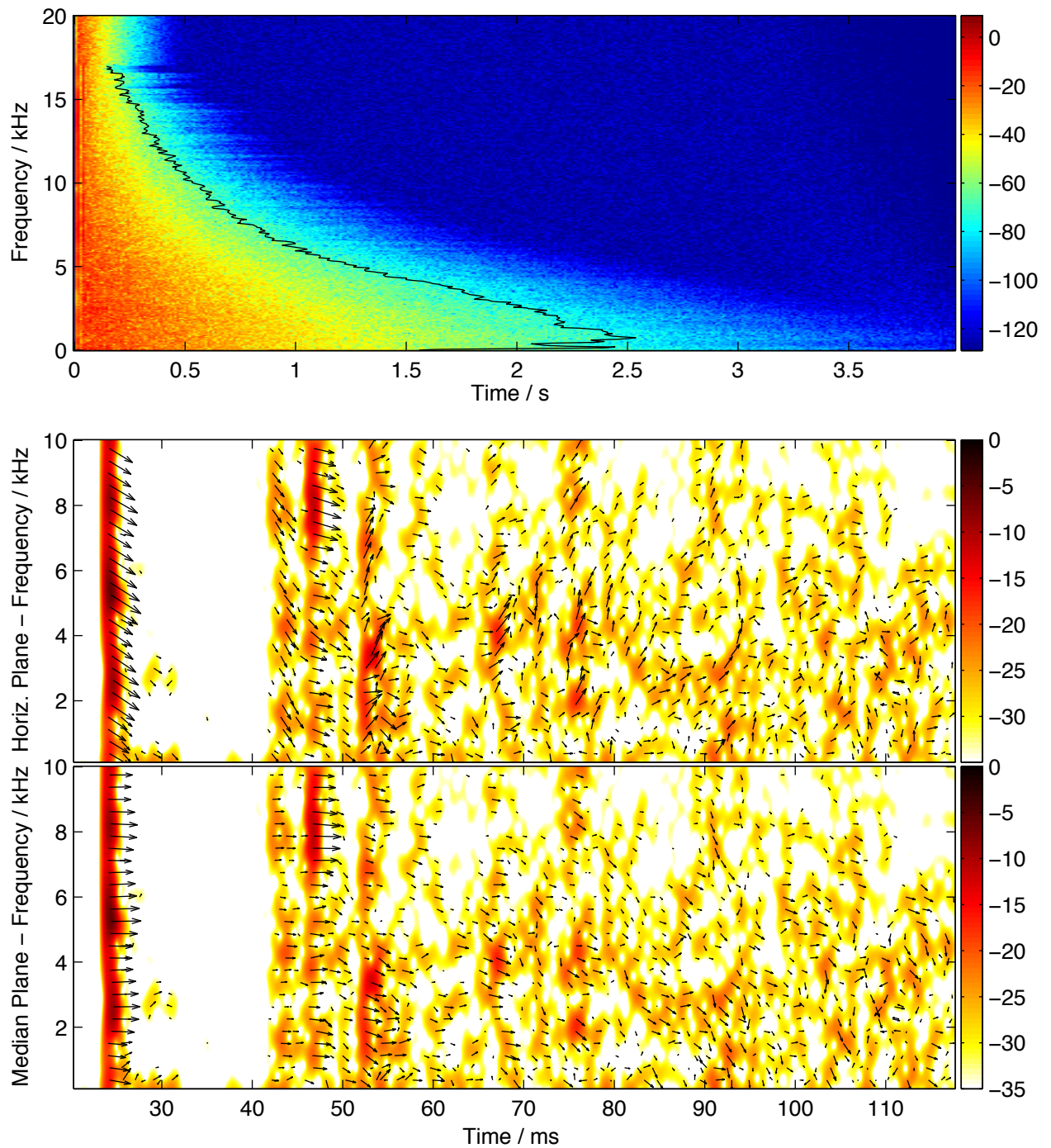
S1–R4

	125 Hz	250 Hz	500 Hz	1 kHz	2 kHz	4 kHz	8 kHz
T_{30} (s)	2.7	2.5	2.5	2.4	2.1	1.8	1.2
EDT (s)	2.6	2.4	2.5	2.5	2.1	1.6	1.0
G (dB)	6.5	8.4	7.6	8.0	8.1	6.0	-0.4
C_{80} (dB)	-4.9	-1.9	-2.7	-1.9	-1.6	0.6	3.5
$1 - \text{IACC}_E$	0.07	0.22	0.86	0.71	0.74	0.75	-
$1 - \text{IACC}_L$	0.09	0.28	0.84	0.96	0.95	0.91	-
LF_P	0.12	0.15	0.29	0.29	0.29	0.33	-
LF_{SF}	0.27	0.26	0.29	0.27	0.42	0.63	-
SNR (dB)	65.2	65.8	67.0	68.4	71.0	67.6	59.8



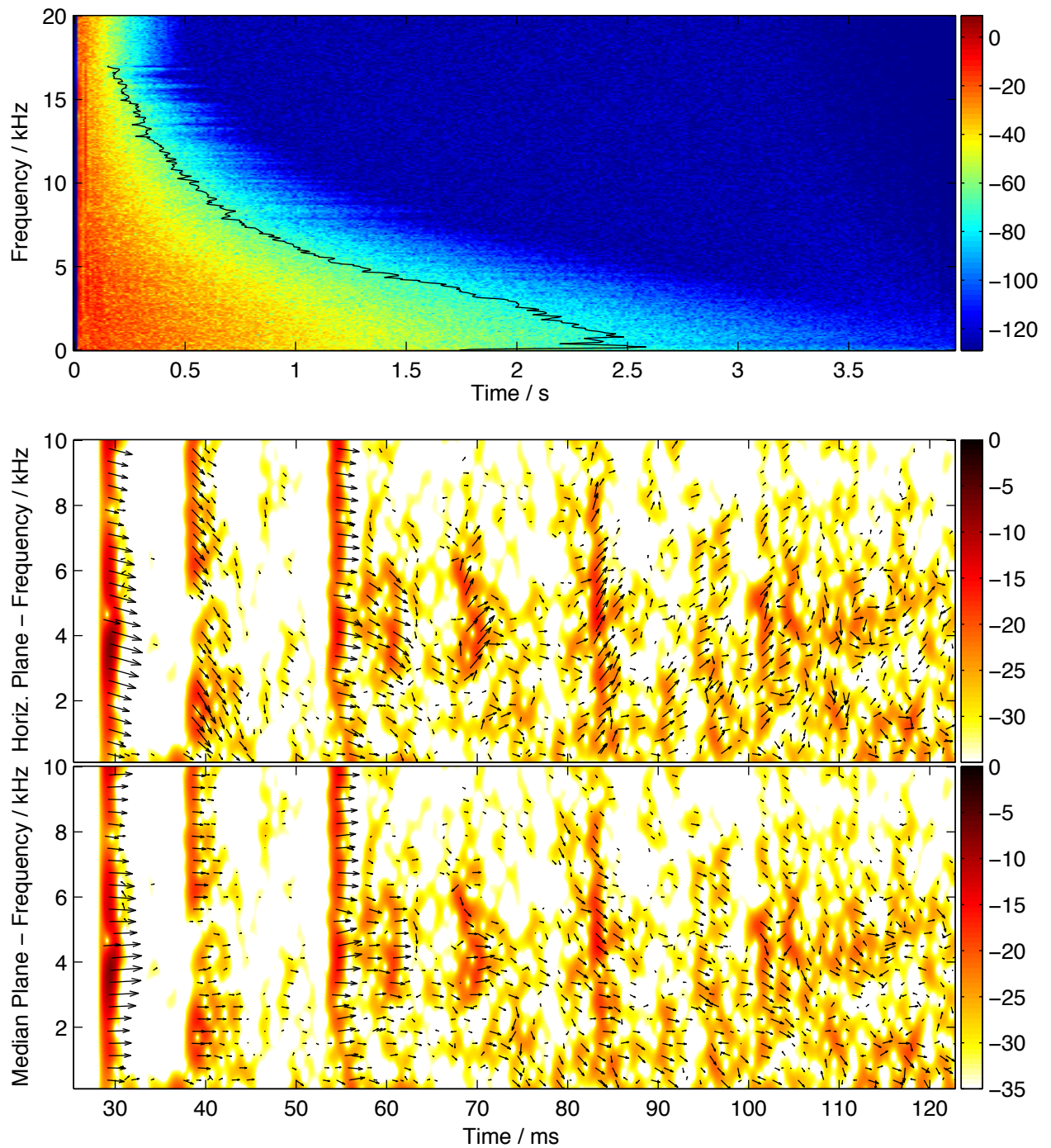
S2–R1

	125 Hz	250 Hz	500 Hz	1 kHz	2 kHz	4 kHz	8 kHz
T_{30} (s)	2.6	2.4	2.4	2.4	2.1	1.7	1.1
EDT (s)	2.0	2.1	2.5	2.4	2.0	1.6	0.8
G (dB)	10.9	10.1	9.1	9.2	9.8	8.0	5.7
C_{80} (dB)	0.2	-3.2	-3.1	-3.7	-2.4	-0.1	7.6
$1 - \text{IACC}_E$	0.14	0.28	0.79	0.61	0.83	0.79	-
$1 - \text{IACC}_L$	0.09	0.26	0.80	0.86	0.92	0.94	-
LF_P	0.22	0.27	0.25	0.53	0.46	0.56	-
LF_{SF}	0.37	0.37	0.27	0.50	0.72	0.77	-
SNR (dB)	66.6	61.6	66.8	69.1	69.5	70.0	71.3



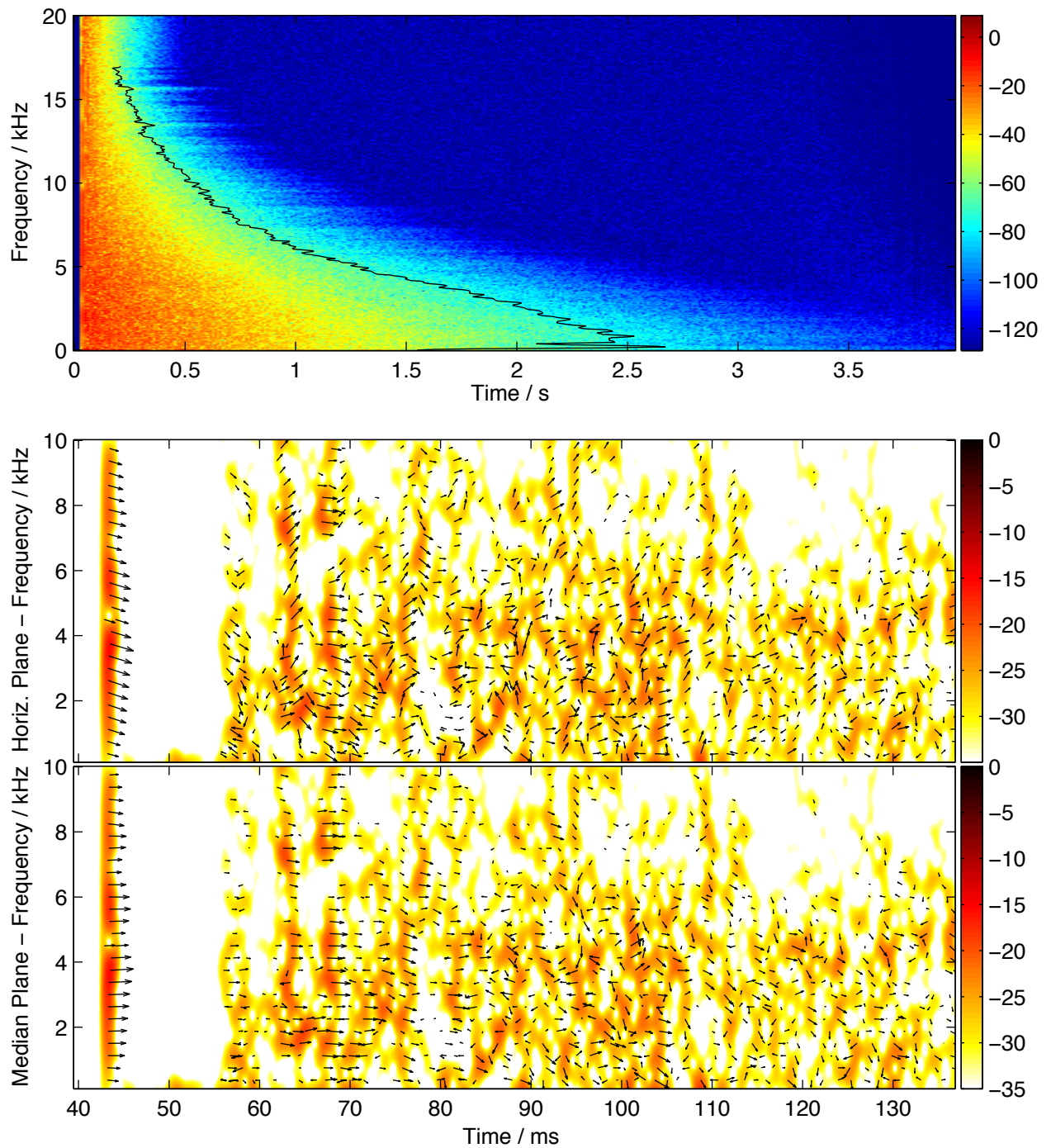
S2–R2

	125 Hz	250 Hz	500 Hz	1 kHz	2 kHz	4 kHz	8 kHz
T_{30} (s)	2.6	2.4	2.3	2.4	2.1	1.7	1.2
EDT (s)	2.2	2.4	2.5	2.3	2.0	1.4	0.9
G (dB)	9.2	9.4	8.9	9.6	10.1	9.7	4.1
C_{80} (dB)	-2.8	-6.1	-4.8	-2.9	-1.4	2.2	5.6
$1 - \text{IACC}_E$	0.19	0.24	0.81	0.73	0.76	0.70	-
$1 - \text{IACC}_L$	0.15	0.30	0.88	0.91	0.95	0.96	-
LF_P	0.52	0.14	0.27	0.40	0.36	0.33	-
LF_{SF}	0.46	0.29	0.28	0.39	0.48	0.39	-
SNR (dB)	67.1	68.9	65.0	69.5	75.5	74.6	70.0



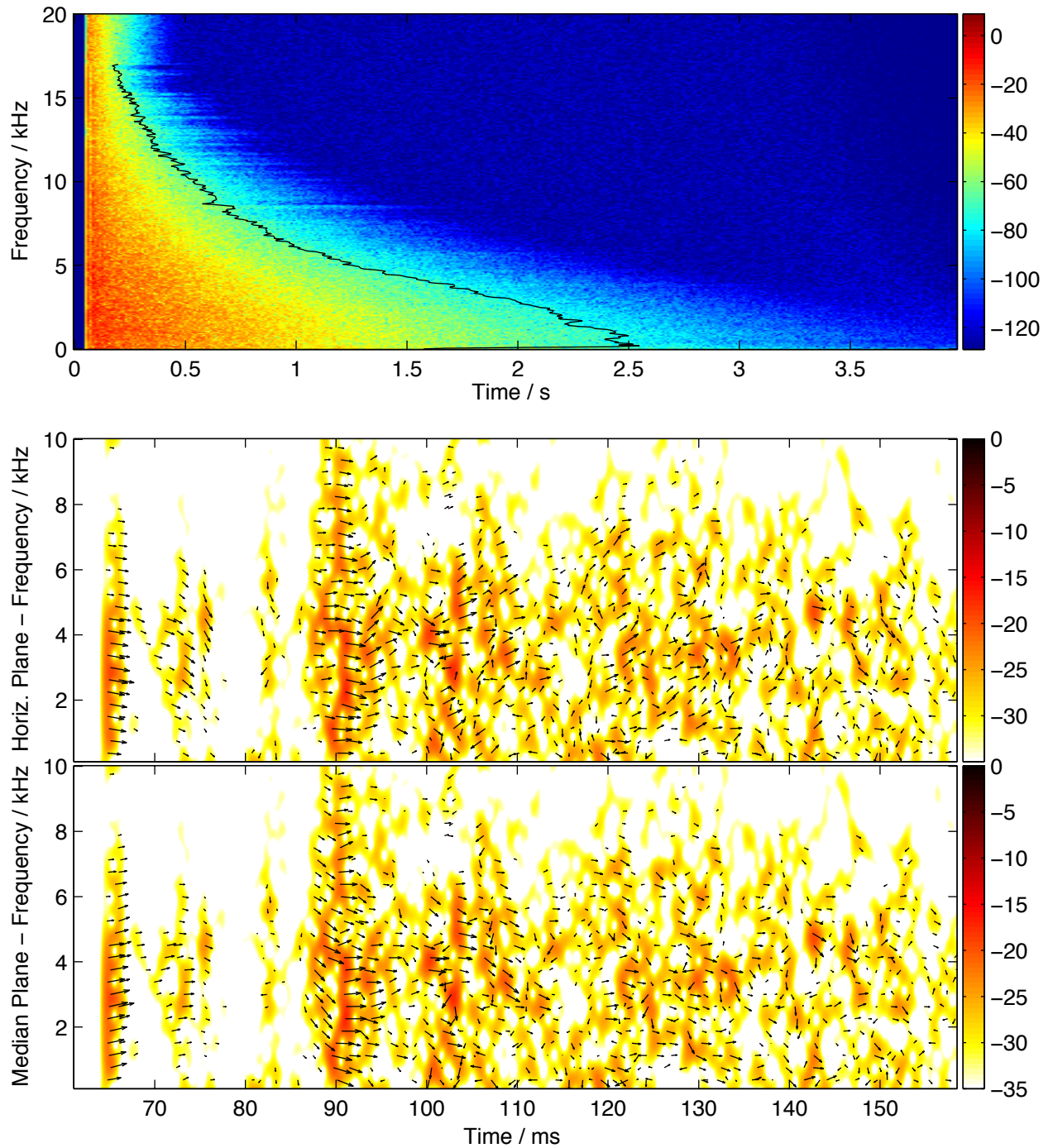
S2–R3

	125 Hz	250 Hz	500 Hz	1 kHz	2 kHz	4 kHz	8 kHz
T_{30} (s)	2.7	2.5	2.4	2.4	2.1	1.7	1.2
EDT (s)	3.0	2.8	2.4	2.3	2.0	1.6	1.0
G (dB)	7.5	7.1	8.5	9.1	9.5	7.0	2.7
C_{80} (dB)	0.2	-3.8	-4.4	-2.4	-0.6	-0.1	5.5
$1 - \text{IACC}_E$	0.08	0.20	0.71	0.81	0.69	0.71	-
$1 - \text{IACC}_L$	0.10	0.33	0.84	0.85	0.96	0.95	-
LF_P	0.25	0.21	0.51	0.57	0.28	0.41	-
LF_{SF}	0.50	0.24	0.41	0.36	0.59	0.63	-
SNR (dB)	58.3	64.6	63.2	67.6	70.2	69.8	67.5



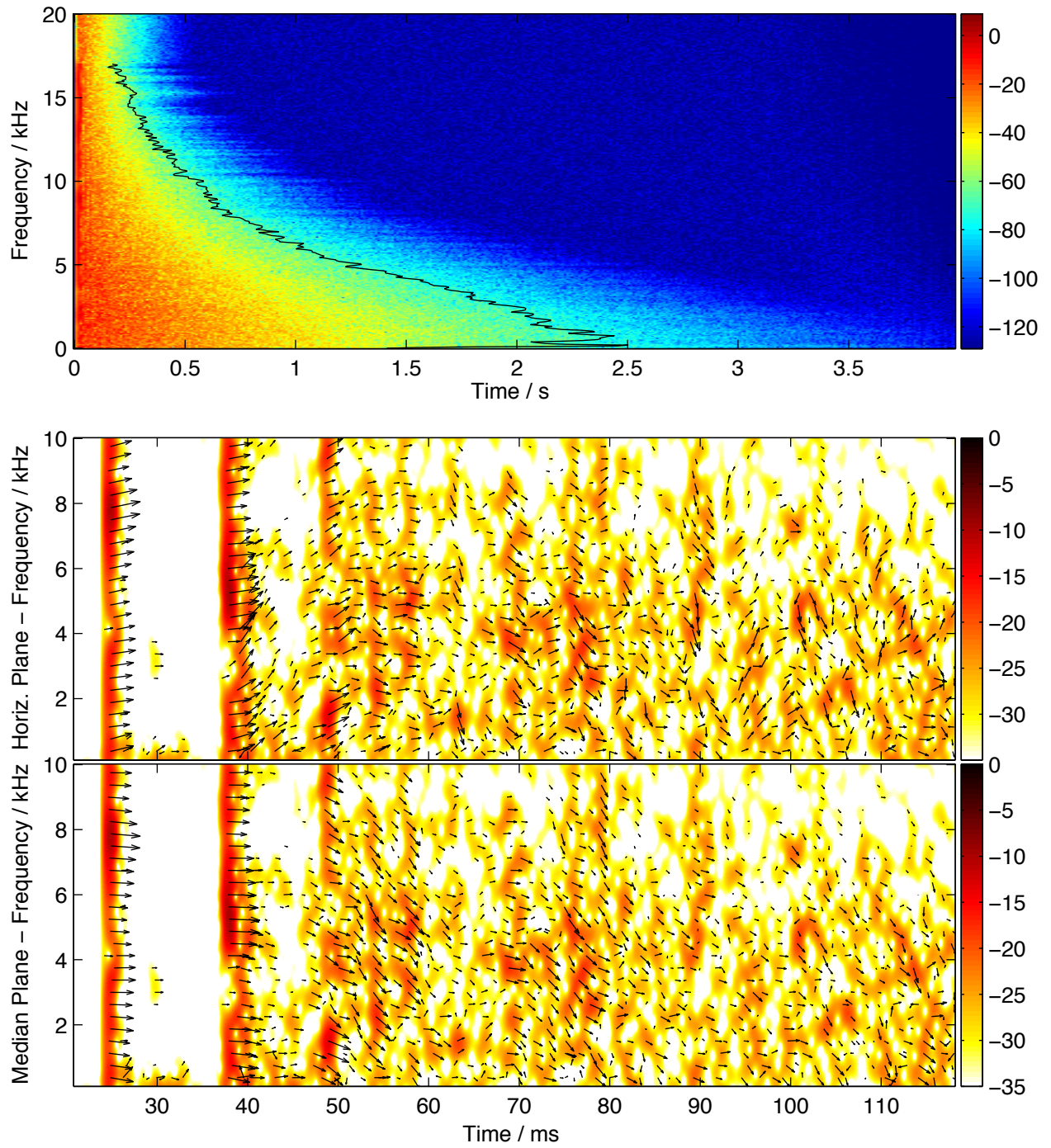
S2–R4

	125 Hz	250 Hz	500 Hz	1 kHz	2 kHz	4 kHz	8 kHz
T_{30} (s)	2.8	2.6	2.4	2.3	2.1	1.8	1.2
EDT (s)	2.7	2.3	2.5	2.3	2.1	1.6	0.9
G (dB)	6.8	7.9	7.8	8.6	8.5	6.2	-0.0
C_{80} (dB)	-6.7	-3.2	-2.4	-2.1	-0.4	1.5	4.5
$1 - \text{IACC}_E$	0.04	0.28	0.71	0.89	0.76	0.87	-
$1 - \text{IACC}_L$	0.08	0.23	0.90	0.85	0.95	0.94	-
LF_P	0.15	0.33	0.21	0.33	0.28	0.39	-
LF_{SF}	0.31	0.44	0.34	0.28	0.40	0.56	-
SNR (dB)	66.7	64.8	65.7	69.9	73.5	67.0	61.6



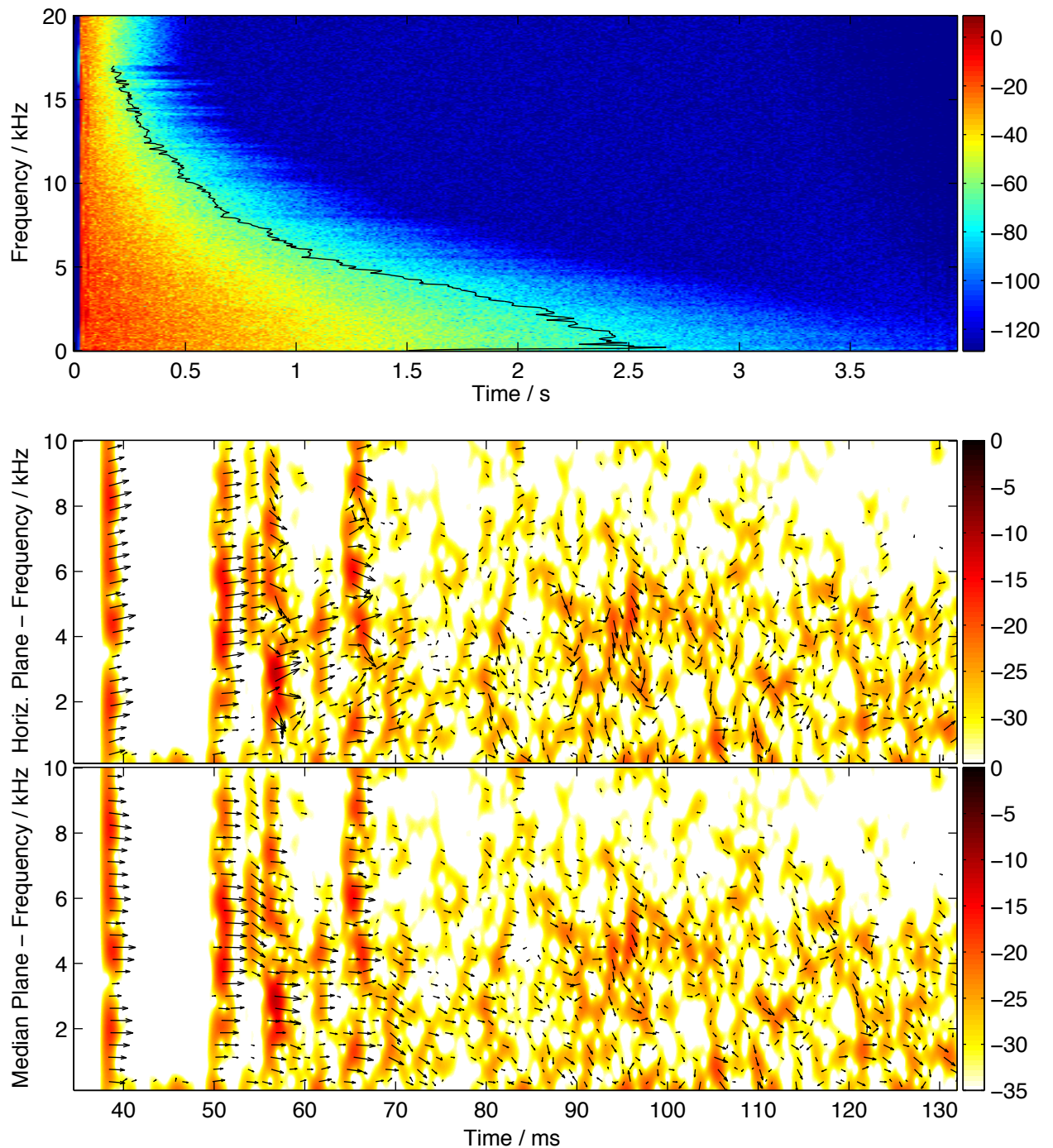
S3–R1

	125 Hz	250 Hz	500 Hz	1 kHz	2 kHz	4 kHz	8 kHz
T_{30} (s)	2.7	2.5	2.4	2.4	2.1	1.7	1.1
EDT (s)	2.8	2.4	2.4	2.3	2.0	1.6	0.8
G (dB)	9.4	9.2	9.9	10.0	10.7	8.4	6.2
C_{80} (dB)	2.2	-2.9	-2.6	-1.5	-0.8	0.4	8.0
$1 - \text{IACC}_E$	0.16	0.24	0.54	0.72	0.79	0.79	-
$1 - \text{IACC}_L$	0.18	0.31	0.91	0.87	0.92	0.94	-
LF_P	0.36	0.20	0.17	0.37	0.37	0.46	-
LF_{SF}	0.38	0.20	0.21	0.44	0.47	0.47	-
SNR (dB)	64.9	62.0	65.3	64.1	72.8	73.5	73.9



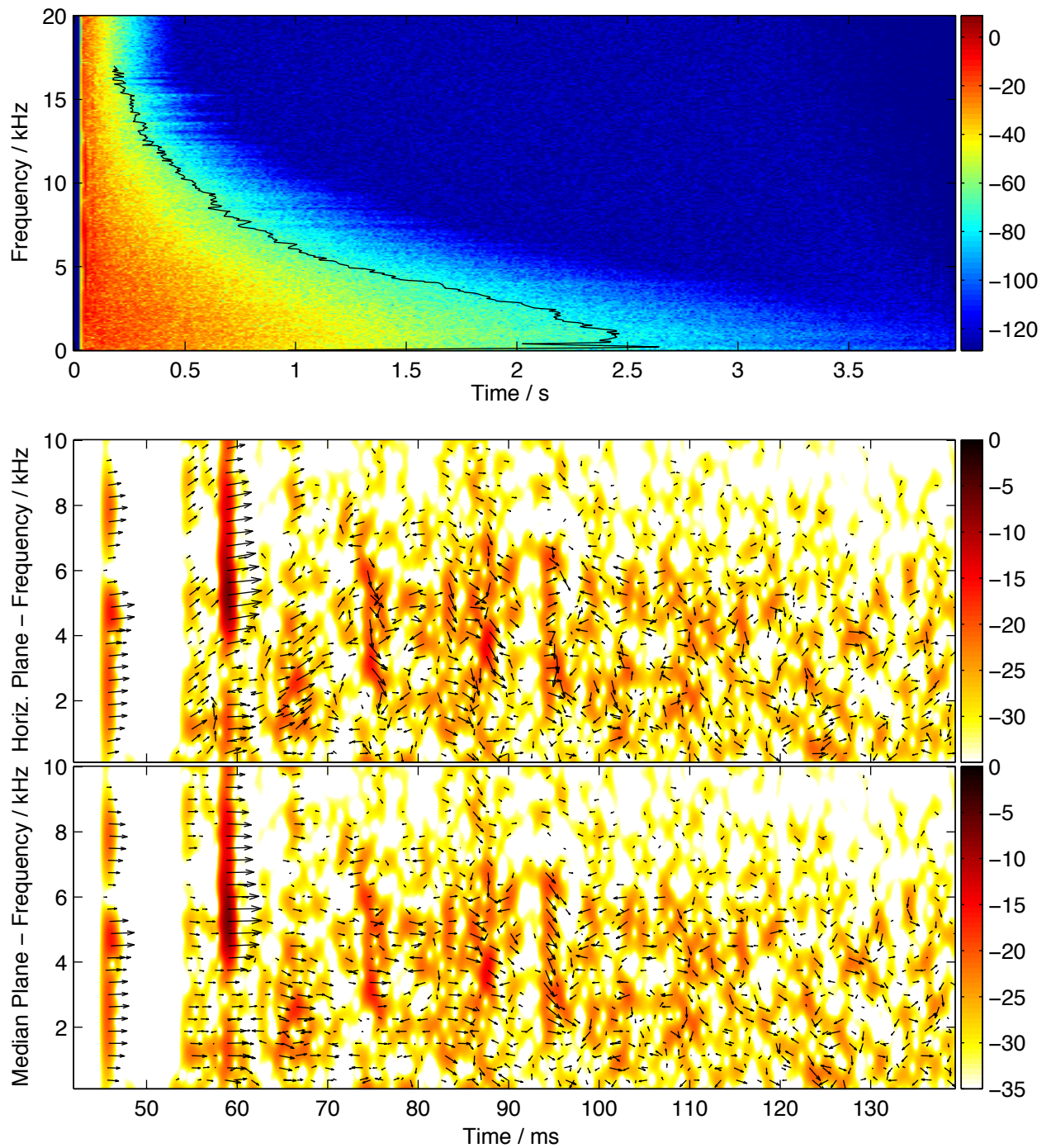
S3–R2

	125 Hz	250 Hz	500 Hz	1 kHz	2 kHz	4 kHz	8 kHz
T_{30} (s)	2.7	2.5	2.4	2.4	2.1	1.7	1.2
EDT (s)	2.3	2.3	2.5	2.2	2.0	1.5	0.9
G (dB)	9.8	8.7	8.7	9.5	10.6	9.2	3.5
C_{80} (dB)	-1.2	-2.5	-3.8	-3.1	0.8	3.3	6.3
$1 - \text{IACC}_E$	0.07	0.20	0.82	0.75	0.73	0.65	-
$1 - \text{IACC}_L$	0.09	0.34	0.91	0.91	0.90	0.96	-
LF_P	0.19	0.20	0.30	0.44	0.29	0.46	-
LF_{SF}	0.34	0.50	0.49	0.53	0.48	0.44	-
SNR (dB)	68.4	67.5	66.2	69.3	76.8	77.3	67.6



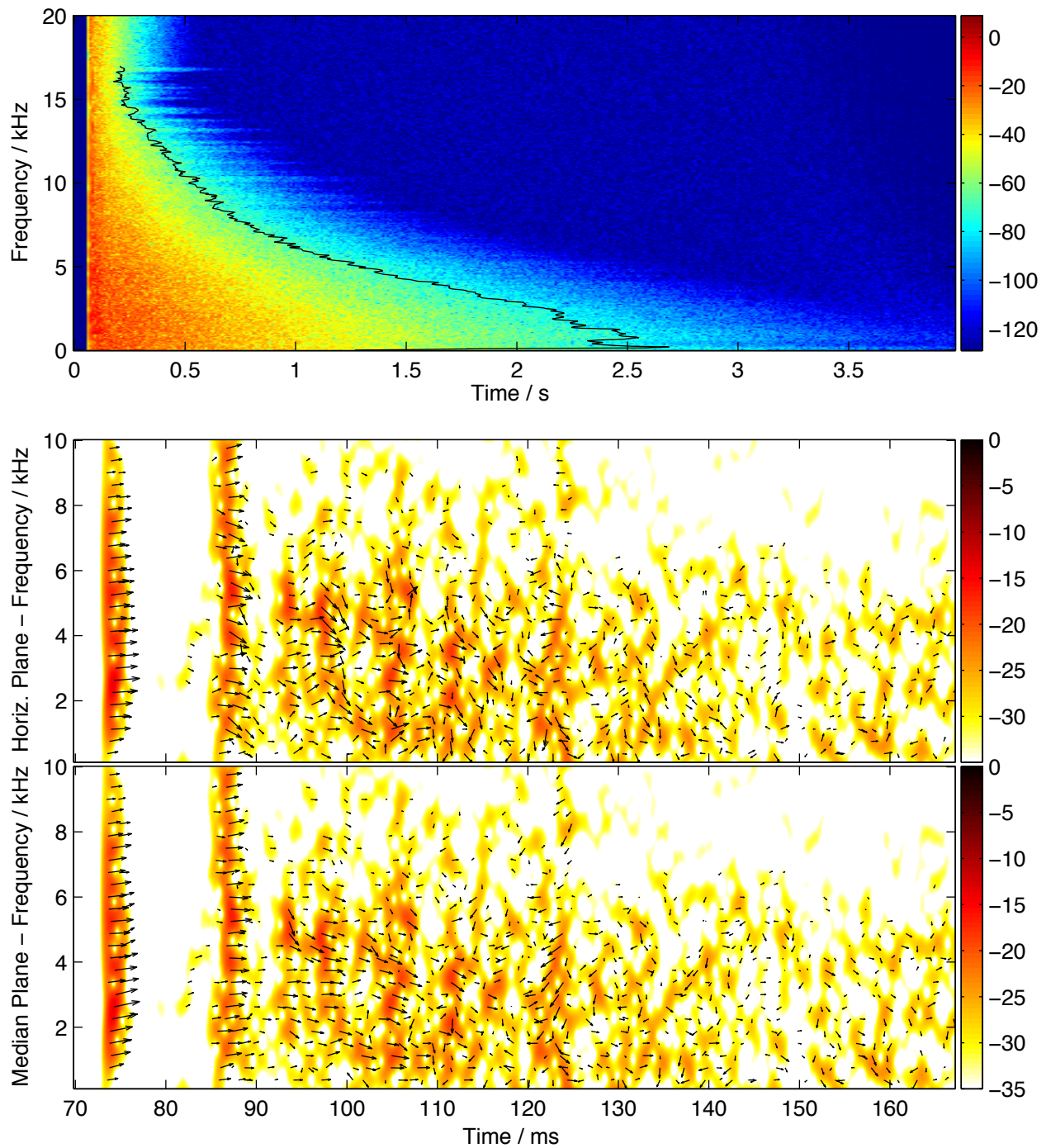
S3–R3

	125 Hz	250 Hz	500 Hz	1 kHz	2 kHz	4 kHz	8 kHz
T_{30} (s)	2.8	2.5	2.4	2.4	2.1	1.7	1.2
EDT (s)	2.9	2.7	2.2	2.2	2.0	1.3	0.6
G (dB)	6.9	7.3	8.9	9.6	10.3	9.6	4.9
C_{80} (dB)	-0.3	-5.7	-4.9	-3.3	0.1	4.3	8.4
$1 - \text{IACC}_E$	0.15	0.30	0.77	0.92	0.75	0.80	-
$1 - \text{IACC}_L$	0.15	0.37	0.79	0.92	0.93	0.92	-
LF_P	0.36	0.35	0.34	0.36	0.48	0.29	-
LF_{SF}	0.60	0.44	0.34	0.37	0.65	0.69	-
SNR (dB)	63.9	62.7	66.8	69.2	72.9	79.0	69.5



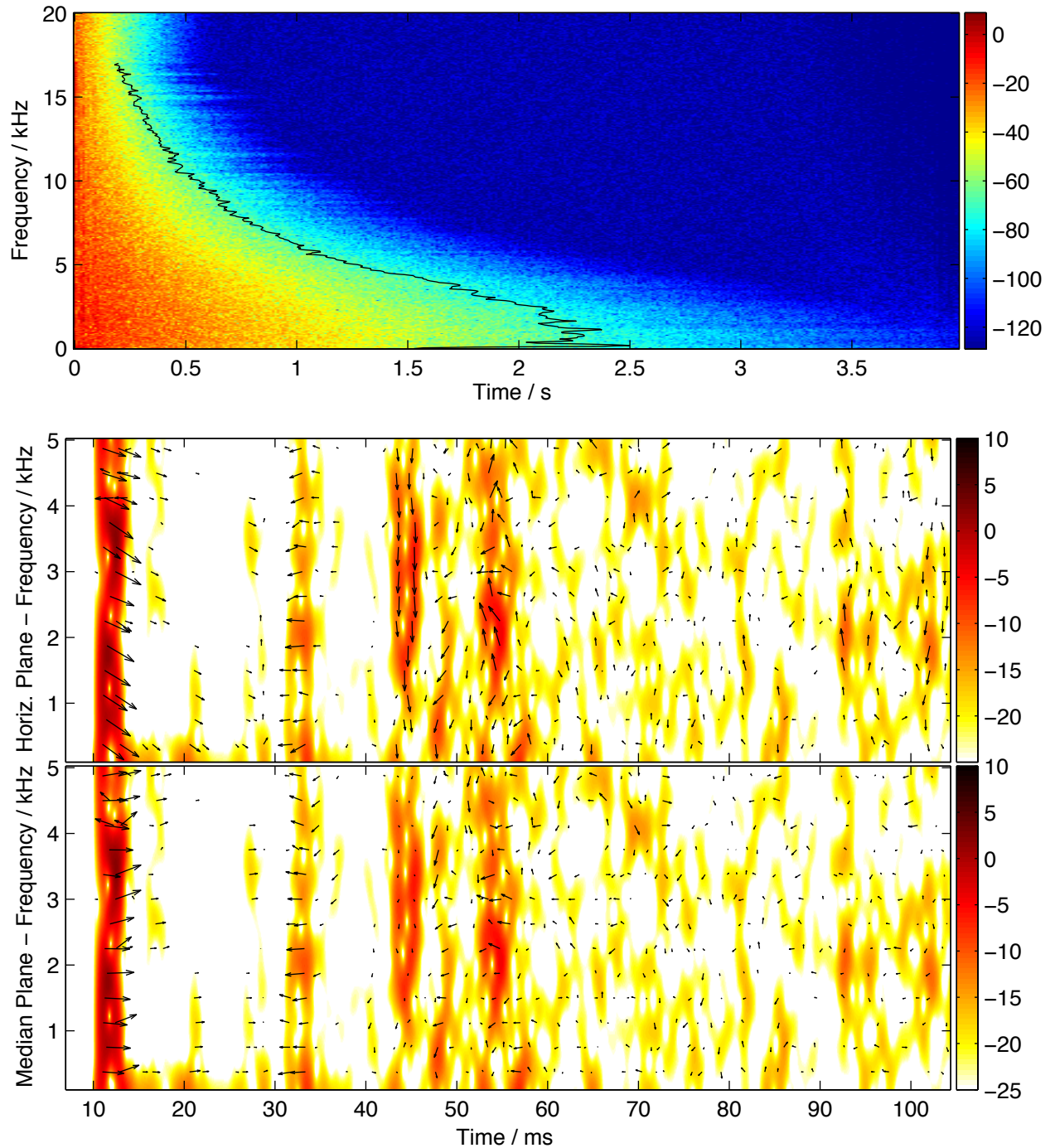
S3–R4

	125 Hz	250 Hz	500 Hz	1 kHz	2 kHz	4 kHz	8 kHz
T_{30} (s)	2.8	2.5	2.4	2.4	2.1	1.7	1.2
EDT (s)	2.8	2.5	2.4	2.2	2.1	1.6	1.0
G (dB)	5.9	7.1	7.9	9.1	8.5	6.1	-0.4
C_{80} (dB)	-2.4	-4.4	-3.2	0.5	0.1	1.7	4.9
$1 - \text{IACC}_E$	0.07	0.32	0.88	0.88	0.84	0.82	-
$1 - \text{IACC}_L$	0.14	0.43	0.85	0.95	0.94	0.91	-
LF_P	0.17	0.29	0.37	0.24	0.30	0.45	-
LF_{SF}	0.40	0.48	0.55	0.41	0.40	0.66	-
SNR (dB)	62.0	64.7	66.8	69.3	68.7	66.2	59.1



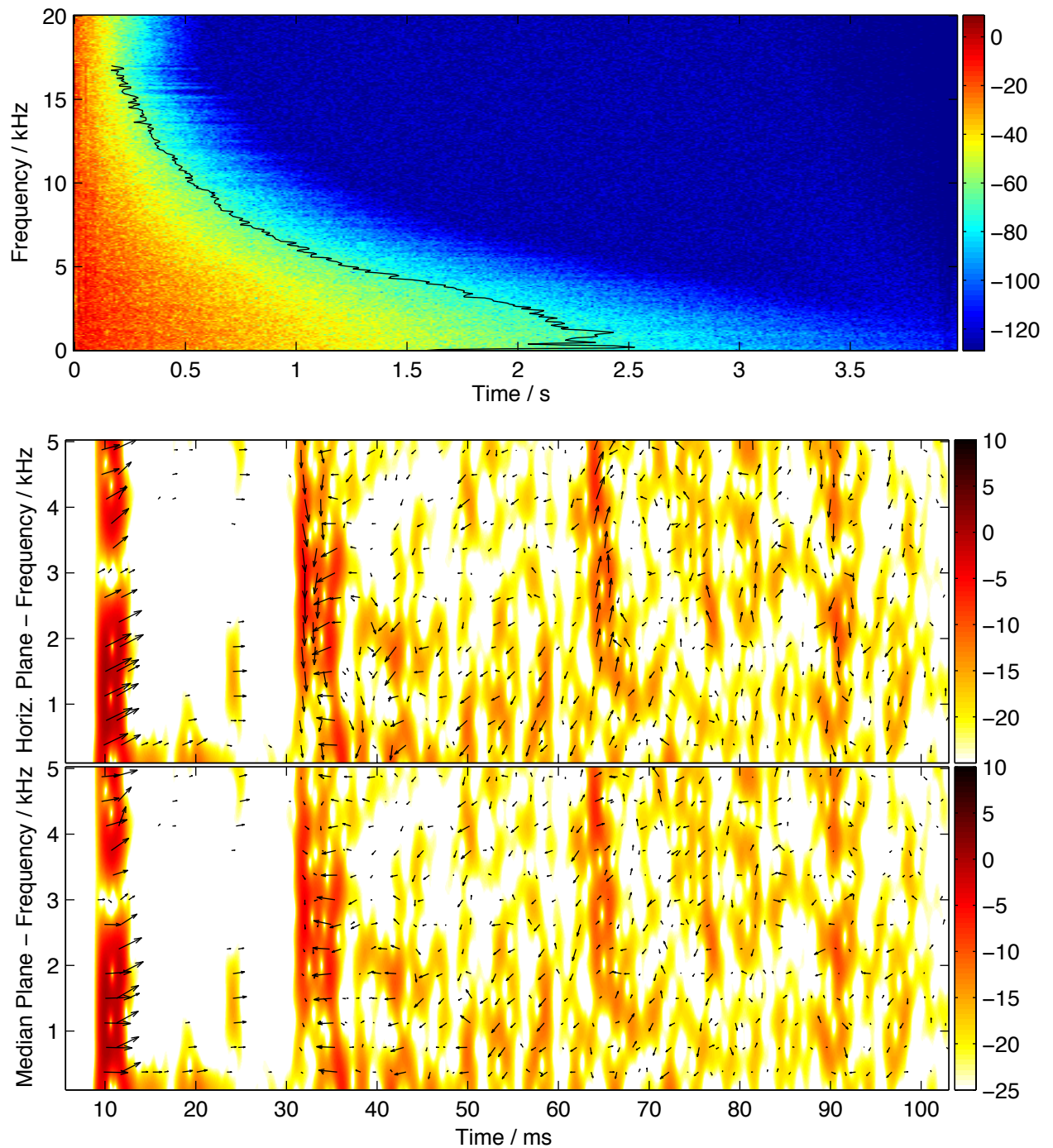
S1-P1

	125 Hz	250 Hz	500 Hz	1 kHz	2 kHz	4 kHz	8 kHz
T_{30} (s)	2.6	2.5	2.4	2.4	2.1	1.7	1.1
EDT (s)	1.2	1.6	2.3	2.1	1.8	1.5	0.8
G (dB)	14.9	13.9	14.0	14.6	14.7	12.8	11.6
C_{80} (dB)	5.6	1.6	1.5	2.3	2.5	4.2	11.4
SNR (dB)	72.1	69.9	73.1	77.8	78.8	77.7	79.8



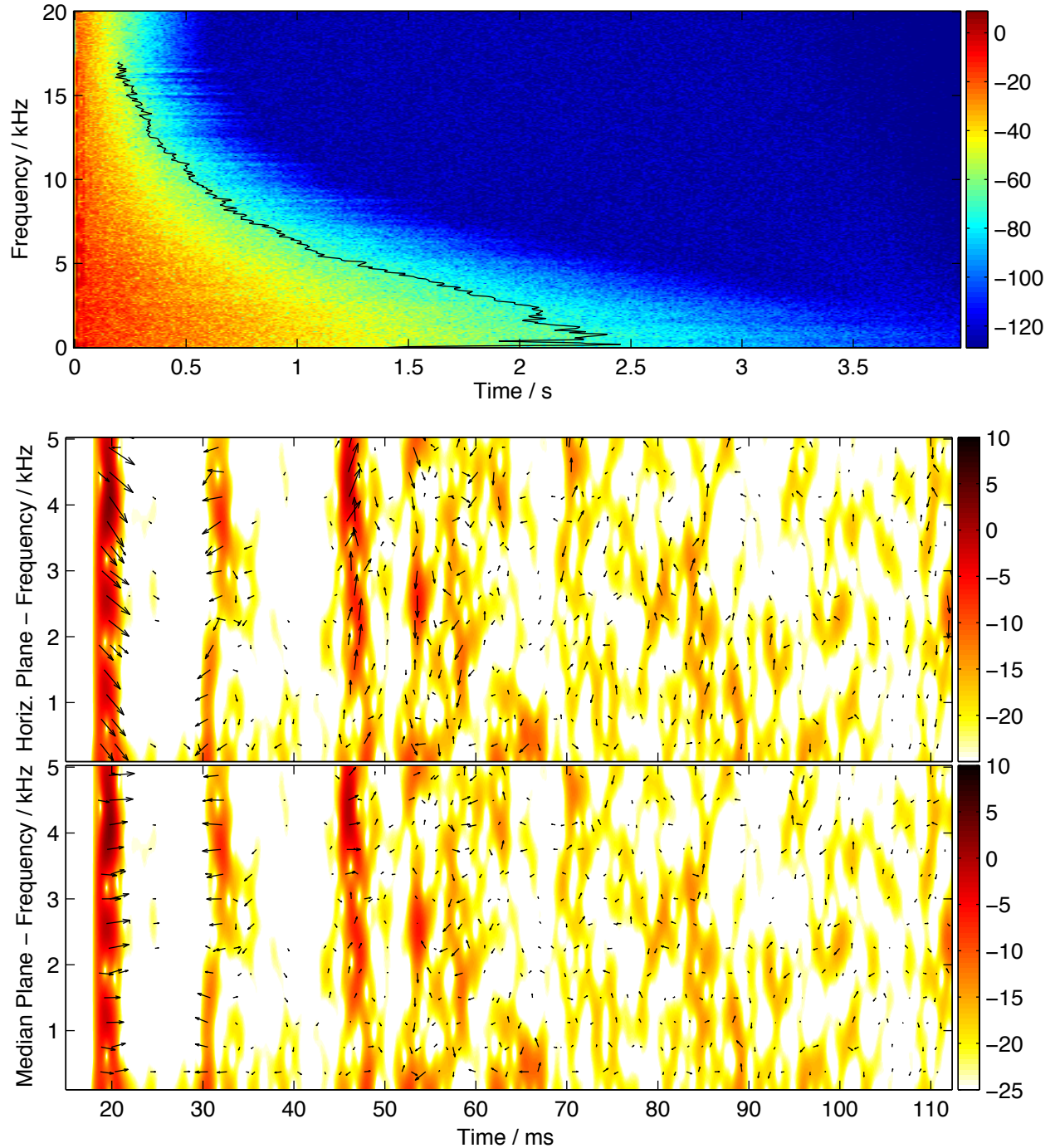
S1-P2

	125 Hz	250 Hz	500 Hz	1 kHz	2 kHz	4 kHz	8 kHz
T_{30} (s)	2.6	2.5	2.4	2.3	2.1	1.7	1.1
EDT (s)	1.7	2.0	1.9	1.9	1.6	1.4	0.7
G (dB)	13.7	13.8	15.6	15.5	15.3	12.2	12.9
C_{80} (dB)	5.1	1.6	3.4	2.7	3.4	3.2	12.4
SNR (dB)	75.0	69.1	74.2	79.5	76.9	75.7	79.8



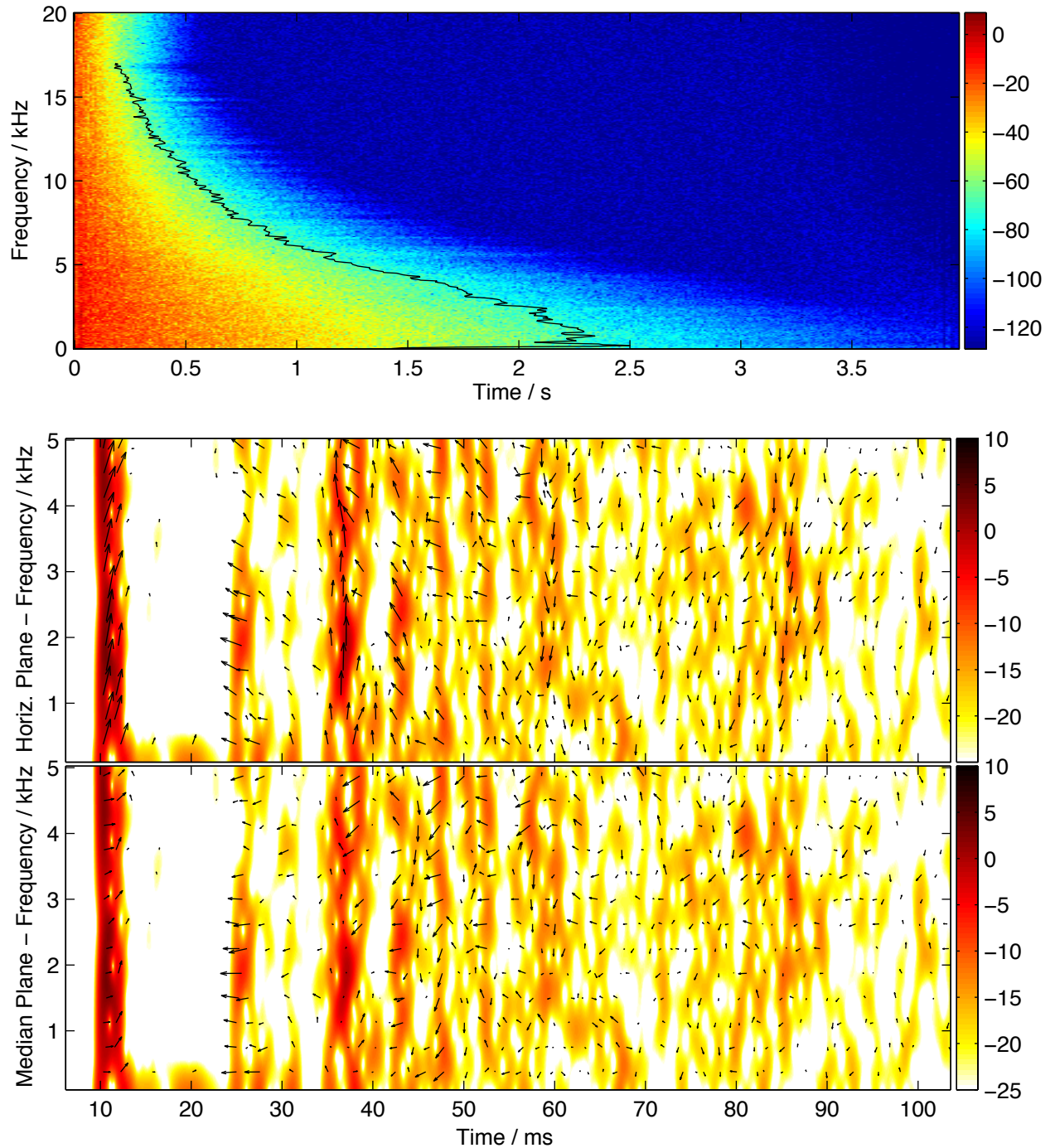
S1–P3

	125 Hz	250 Hz	500 Hz	1 kHz	2 kHz	4 kHz	8 kHz
T_{30} (s)	2.4	2.5	2.5	2.3	2.1	1.7	1.1
EDT (s)	1.6	1.4	2.2	2.1	1.8	1.3	0.6
G (dB)	14.3	14.9	12.0	13.4	13.8	13.7	9.0
C_{80} (dB)	5.1	4.1	-0.3	0.9	2.3	5.9	9.4
SNR (dB)	71.7	69.8	65.6	75.7	77.6	80.6	74.4

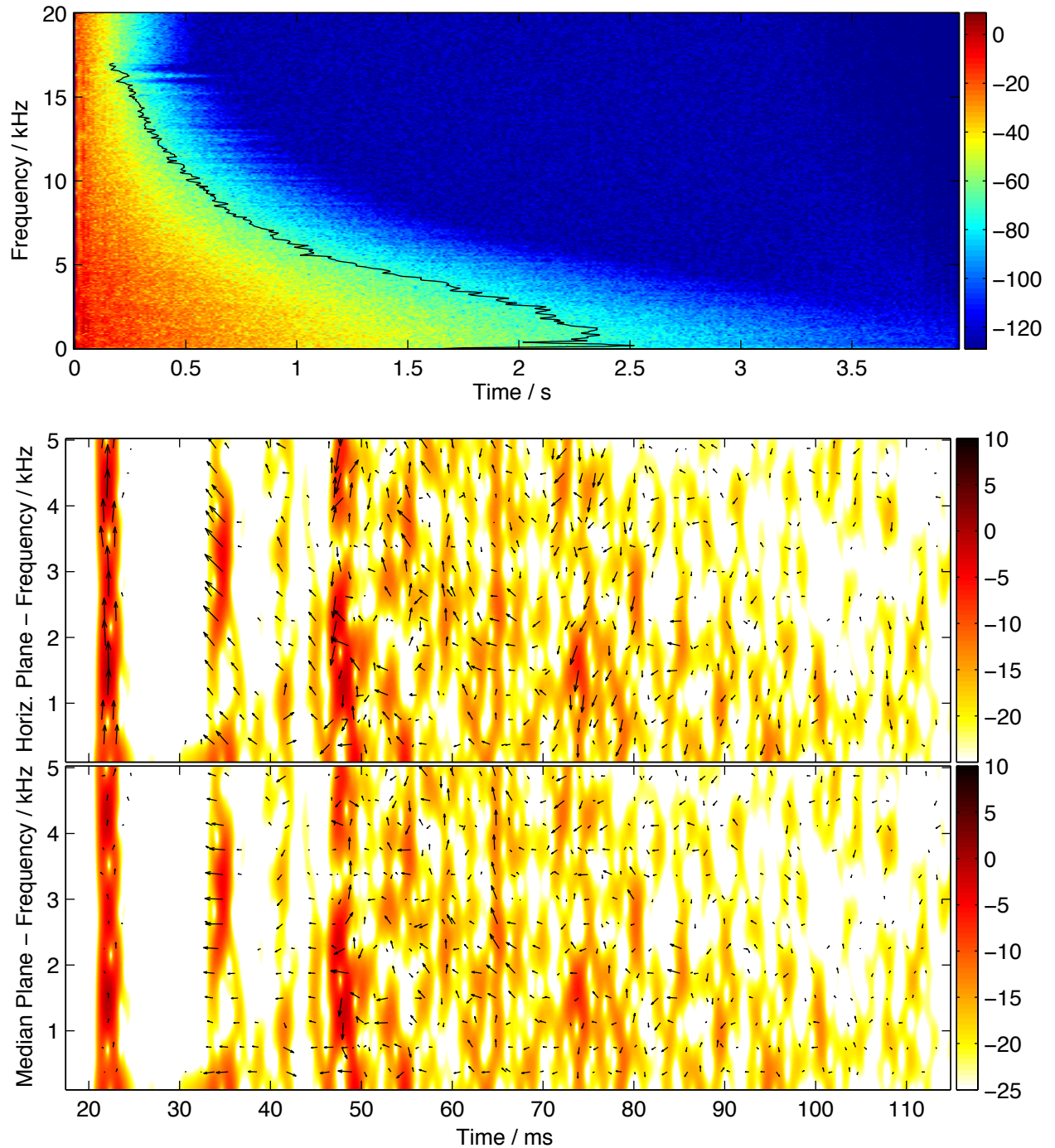


S2–P1

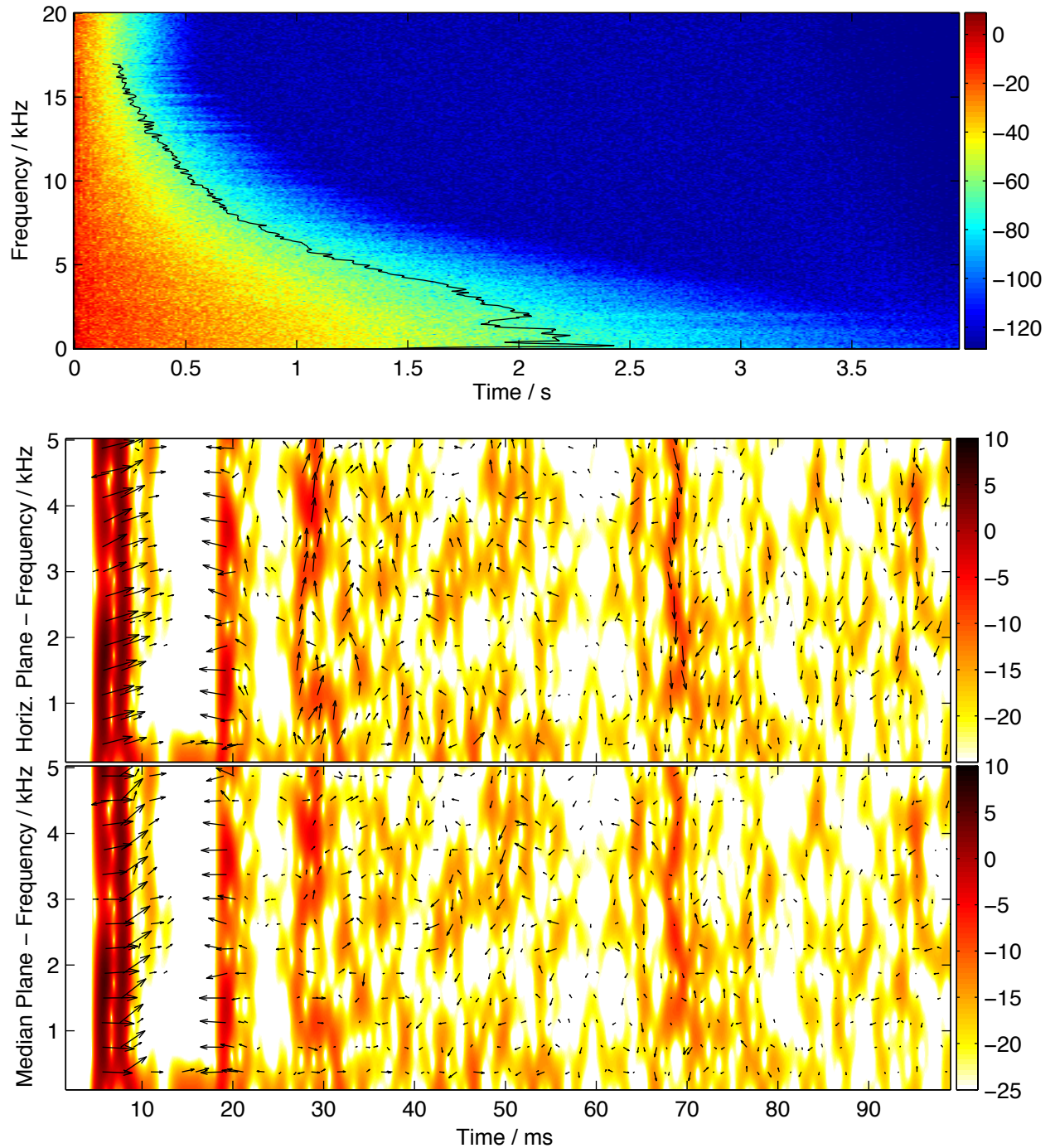
	125 Hz	250 Hz	500 Hz	1 kHz	2 kHz	4 kHz	8 kHz
T_{30} (s)	2.5	2.4	2.4	2.3	2.1	1.6	1.1
EDT (s)	1.8	1.9	2.1	1.9	1.5	1.3	0.8
G (dB)	14.8	14.8	15.0	15.8	16.6	14.5	10.5
C_{80} (dB)	5.8	3.7	2.8	4.5	5.2	5.5	9.1
SNR (dB)	72.9	69.0	73.9	79.7	80.4	83.0	77.8



	125 Hz	250 Hz	500 Hz	1 kHz	2 kHz	4 kHz	8 kHz
T_{30} (s)	2.7	2.3	2.3	2.3	2.1	1.7	1.1
EDT (s)	1.6	1.7	1.9	1.7	1.7	1.3	0.8
G (dB)	14.3	16.3	13.9	15.4	14.5	12.6	6.8
C_{80} (dB)	5.9	3.1	-0.3	2.4	3.0	4.0	6.8
SNR (dB)	70.7	72.2	64.5	77.7	74.1	75.2	70.2

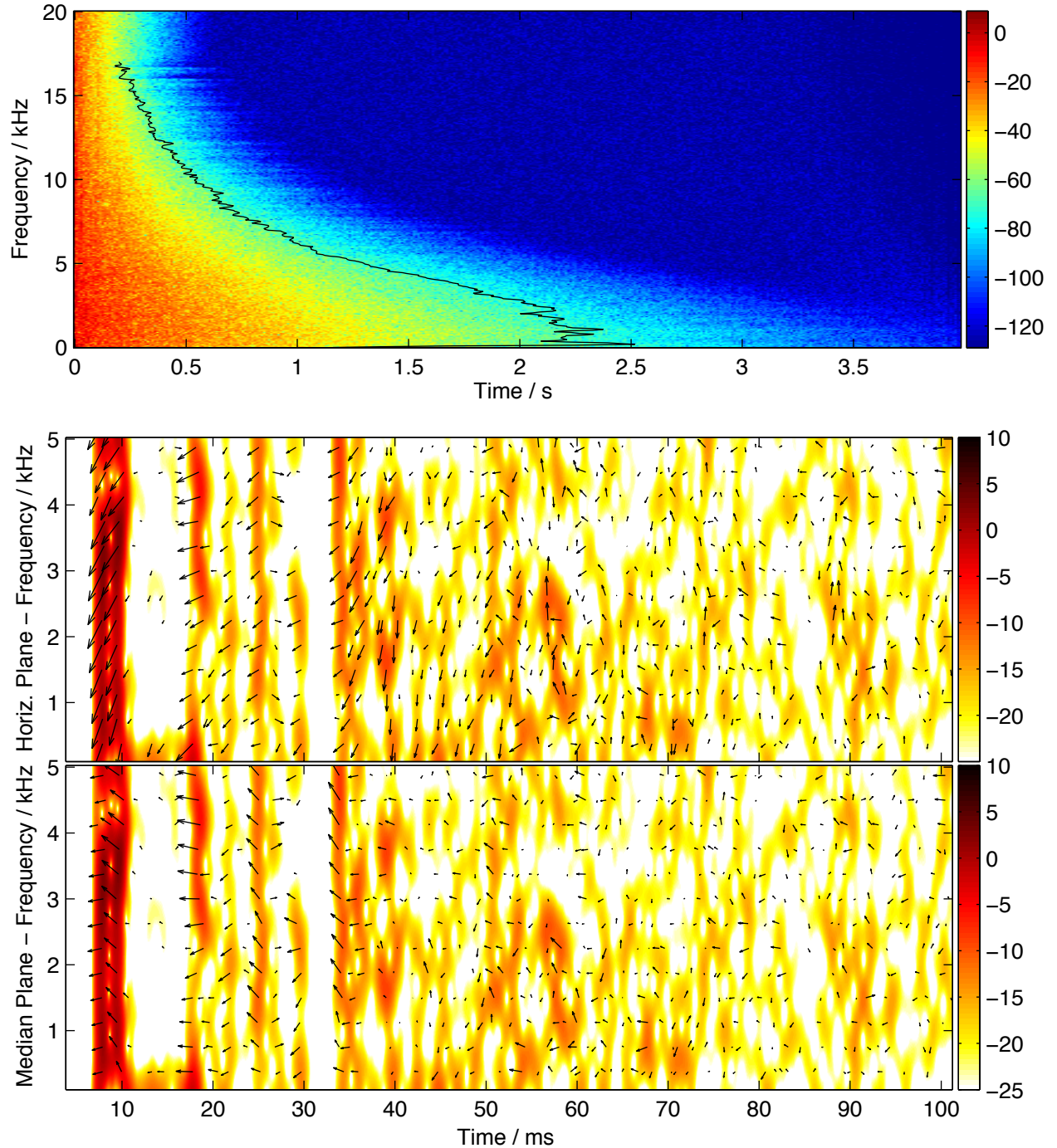


	125 Hz	250 Hz	500 Hz	1 kHz	2 kHz	4 kHz	8 kHz
T_{30} (s)	2.5	2.5	2.4	2.3	2.1	1.6	1.0
EDT (s)	1.5	1.6	1.4	1.4	1.3	1.0	0.0
G (dB)	16.2	16.0	18.3	17.9	18.8	17.3	16.5
C_{80} (dB)	6.4	4.2	7.5	6.8	8.0	8.8	15.8
SNR (dB)	73.3	72.1	75.5	81.6	83.0	84.1	85.1



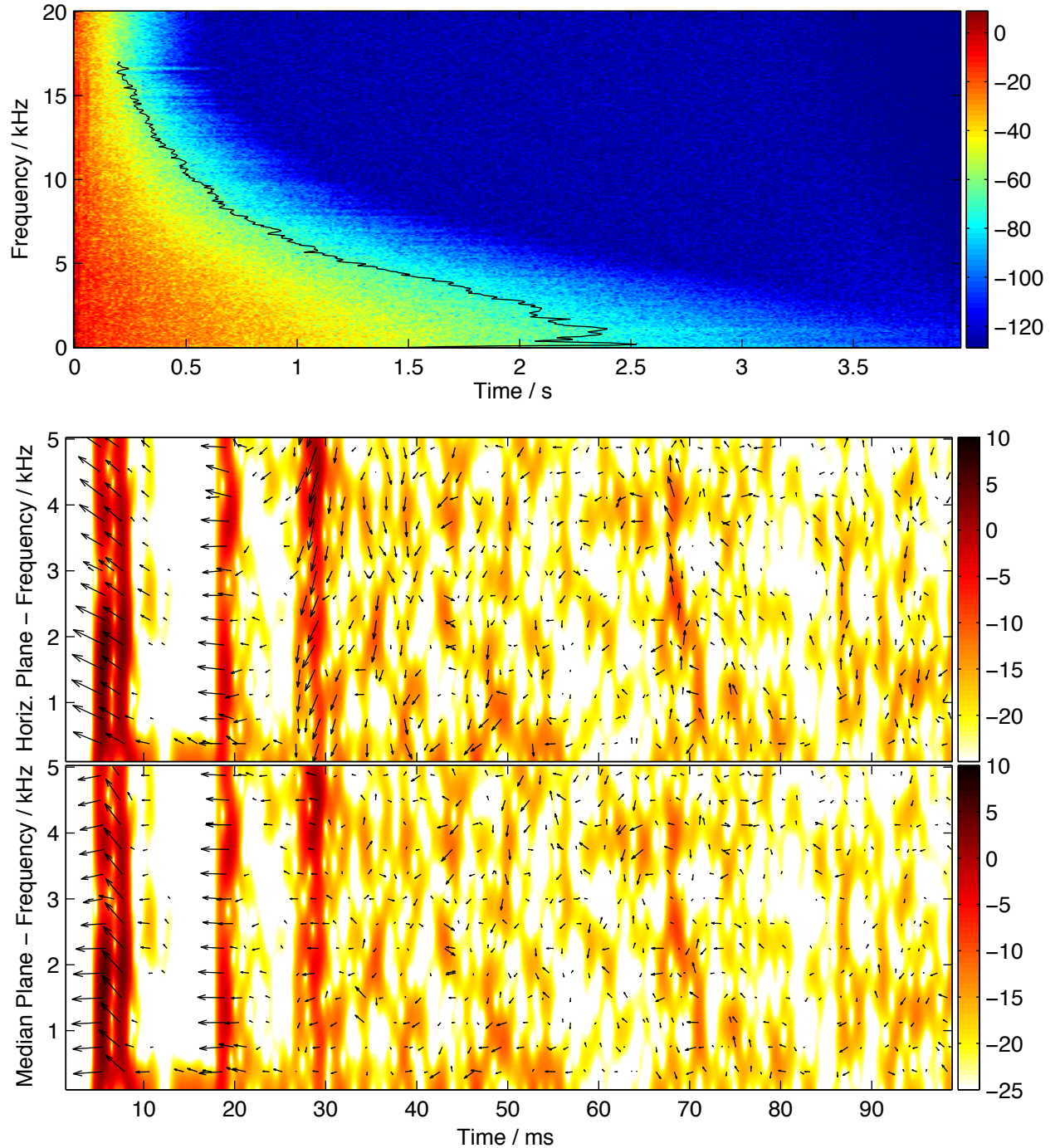
S3–P1

	125 Hz	250 Hz	500 Hz	1 kHz	2 kHz	4 kHz	8 kHz
T_{30} (s)	2.4	2.5	2.4	2.3	2.1	1.7	1.1
EDT (s)	1.6	1.7	1.8	2.0	1.7	1.4	0.7
G (dB)	15.8	14.4	16.7	16.1	15.8	14.1	10.2
C_{80} (dB)	5.8	3.7	5.4	4.5	4.2	5.5	9.6
SNR (dB)	73.7	68.3	75.4	79.9	83.0	79.5	75.3



S3–P2

	125 Hz	250 Hz	500 Hz	1 kHz	2 kHz	4 kHz	8 kHz
T_{30} (s)	2.6	2.4	2.4	2.4	2.0	1.6	1.1
EDT (s)	1.2	1.4	1.7	1.4	1.4	1.0	0.6
G (dB)	16.3	16.3	18.1	17.8	18.3	15.8	12.5
C_{80} (dB)	6.9	3.9	7.0	6.5	7.2	7.3	11.9
SNR (dB)	75.9	74.6	76.3	84.1	82.7	80.4	78.9



S3-P3

	125 Hz	250 Hz	500 Hz	1 kHz	2 kHz	4 kHz	8 kHz
T_{30} (s)	2.4	2.2	2.3	2.3	2.1	1.7	1.1
EDT (s)	2.1	2.0	1.8	2.0	1.7	1.5	0.7
G (dB)	15.2	16.4	15.8	15.3	14.5	12.3	8.3
C_{80} (dB)	0.3	1.8	2.3	3.0	2.4	3.4	8.3
SNR (dB)	68.6	72.6	68.9	76.5	75.4	78.8	72.4

